Investigating the role of the Dendritic Cell Immunoactivating Receptor in the Immune Response during *Pneumocystis murina*

by

Nontobeko F. Mthembu

MTHNON042

SUBMITTED TO THE UNIVERSITY OF CAPE TOWN

In fulfilment of the requirements for the degree

MSc (Med) Clinical Science & Immunology

Faculty Health Sciences

UNIVERSITY OF CAPE TOWN

October 2019

Dr J. Claire Hoving

Dr Mohlopheni J. Marakalala

DECLARATION

I, *…Nontobeko Mthembu.....* , hereby declare that the work on which this dissertation/thesis is based is my original work (except where acknowledgements indicate otherwise) and that neither the whole work nor any part of it has been, is being, or is to be submitted for another degree in this or any other university.

I empower the university to reproduce for the purpose of research either the whole or any portion of the contents in any manner whatsoever.

Signature: Signed by candidate……

Date: …07/10/2019……..

Acknowledgements

I would like to thank my supervisor Dr Claire Hoving for giving me the opportunity to be part of her research group in order to further my studies. To our collaborator Jay Kolls, I would like to express my gratitude for providing us with *Pneumocystis* and the PCR standard. I would like to also acknowledge Georgia for her assistance in setting up the *Pneumocystis* standard. To Sho Yamasaki, our collaborator, thank you for providing the DCAR-deficient mice.

A huge thanks to Patricia, who has not only been an amazing friend but for training me and for being with me every step of the way. I appreciate all the night we spent in the lab, learning and troubleshooting together. The emotional support has been amazing, and for going beyond and making sure that I had food when times were hard. I treasure all the moments we spent together and value your unconditional and consistent support without which I would have lost my sanity by the end of this degree.

I cannot forget the greatest support system of my friends and my mentor who have been cheering me on since day one. To Dr Mohlopheni Marakalala who has served as both my co-supervisor and my mentor, I appreciate the support and for believing in me and always pushing me to do my best. To my friends, thank you for encouraging me to stick it out, I am grateful for the love, the laughs, the tears, the highs and the lows and all the memories we have made together. I will carry the love you have shown with me always.

Thanks to National Research Foundation, University of Cape Town and the South African Medical Research Council for funding this research. A huge thank you to the AFGrica Unit and the Institute of Infectious Disease & Molecular Medicine, the institutes which I am part of that have provided the core research facilities. To the animal unit staff, thank you for taking care of my mice.

Finally, I would like to thank my family. To my father, Wiseman Mthembu and my mother Rose Mthembu, I thank God each day for the blessing of having you as my parents. Thank you for always carrying me in prayer and giving me the strength to go forth every time when things seemed impossible. To my

siblings Jabulani, Nonjabulo and Andisiwe, I am grateful for your love and support over the years.

I give thanks to God for the strength and resilience that He so mercifully granted me throughout my studies.

Abstract

Pneumocystis jirovecii causes fungal pneumonia in immunocompromised patients and can be fatal if left untreated. The global mortality rate is estimated to be over 200 000 in AIDS patients. In non-AIDS patients there is an estimated mortality rate of 50 000 cases. This rate is increasing in developed countries, attributed to an increase in disorders which require immunotherapy. These include hematologic malignancies, organ transplant, inflammatory disorders and pre-existing lung disease.

Immediate immunity is initiated by receptors that recognize pathogen associated molecular patterns on the surface of pathogenic fungi. Specifically, C-type lectin receptors (CLRs) have been shown to be the principal initiators of innate immune response during fungal infection. Limited studies have focused on the role of CLRs in *Pneumocystis* infection. Dectin-1and Mincle have been shown to recognise *Pneumocystis* surface antigens with Dectin-1 recognizing β-glucans on the *Pneumocystis* cell wall leading to an effective immune response. However, the role of a newly described CLR, the Dendritic Cell Immunoactivating Receptor (DCAR) remains undefined. For this reason, we investigated the potential role of this receptor in a mouse model of *Pneumocystis murina* infection.

Wild type and DCAR-deficient C57BL/6 mice were infected with *P. murina* organisms via intratracheal instillation. Fungal burden was measured in the lung using quantitative Polymerase Chain Reaction. DCAR-deficient mice had a significantly reduced burden compared to wild type mice at Day 7 and 14 post-infection. To identify the immune components involved in pathogen clearance in these mice we measured cellular recruitment and cytokine production at both early (48 hours) and late (7, 14 and 21 days) time points. Flow cytometry analysis showed an increase in alveolar macrophage, dendritic cells, inflammatory monocytes, eosinophils and T cell recruitment to the lung. While ELISA showed increased levels of IL-1β and IFN-γ at 48 hours, and later on in infection IL-1β and IL-12p40 levels were also elevated. Histology analysis determined the localization of the recruited cells, and

interestingly showed an increase in mucus production at day 21 in DCAR-deficient mice.

In conclusion, we have identified DCAR deficiency as a potential driver of protective immunity in mice during *P. murina* infection. This may be associated with increased levels of IL-1β in DCAR-deficient mice. Furthermore, DCAR may also be important in adaptive inflammatory response regulation, as DCAR-deficient mice have increased cellular recruitment and mucus production later in infection. The mechanism by which the deletion of this receptor affords these mice the ability to efficiently clear *P. murina* remains to be determined.

Key words: *Pneumocystis murina*, C-type lectin receptors, Dendritic Cell Immunoactivating Receptor

Table of Contents

Abbreviations

AMs	Alveolar macrophages
BAL	Bronchoalveolar lavage fluid
BCA	Bicinchoninic Acid Protein Estimation
BSA	Bovine Serum Albumin
cDNA	complementary DNA
CLR	C-type lectin receptor
DCs	Dendritic cells
ELISA	Enzyme-linked immunosorbent assay
FACS	Fluorescence-activated cell sorting
GMS	Grocott's methenamine silver stain
H&E	Haematoxylin and eosin
IFN-γ	Interferon-gamma
IL	Interleukin
IgG	Immunoglobulin G
mRNA	messenger RNA
PAMPs	Pathogen Associated Molecular Patterns
PAS	Periodic acid–Schiff
PRR	Pattern Recognition Receptors
PCP	*Pneumocystis* pneumonia
PCR	Polymerase chain reaction
Rag1	Recombination-activating gene 1
rpm	Revolutions per minute
RT-PCR	Reverse Transcriptase-Polymerase chain reaction
TLR	Toll-like receptor
T cells	T lymphocytes
Th	T helper cells
TNFα	Tumour Necrosis Factor alpha
µm	micrometre
WT	Wild type

List of Figures

Literature Review

Results

List of Tables

Literature Review

Chapter 1: Literature review

1.1. Pneumocystis

The genus *Pneumocystis*, consists of three main species of ubiquitous, yeast-like extracellular fungi which colonize the alveoli of the mammalian lung (1). All three organisms lack attributes of fungal species while concurrently exhibiting characteristics of protozoans, which led to the original classification of *Pneumocystis* as being protozoan (2). However, evidence from DNA sequence analysis demonstrated that this genus, *Pneumocystis*, was in fact an unconventional fungal genus lacking an *in vitro* culture system. Hence, it was later reclassified as fungi. Further genomic analysis revealed a previously unrecognised diversity to be host-specific (2, 3). *Pneumocystis carinii*, for instance, is a rat-specific fungus, whereas pathogenic *Pneumocystis murina* and *Pneumocystis jirovecii* are found in mouse and man, respectively (4). For over 8 decades, the pneumonia causing fungal organism in humans, particularly, immunocompromised hosts, was referred to as *Pneumocystis carinii* (2). Renaming it to *Pneumocystis jirovecii* was inspired by Otto Jirovec, who first described humans as the reservoir host (2).

Within the primary host, *Pneumocystis* undergoes different life stages crucial for survival (Figure 1). Although this has not yet been fully demonstrated due to the inability to culture *Pneumocystis in vitro*, the two main phases in the life cycle of *Pneumocystis* have been reported, namely cystic and trophic forms
(5). In the environment, *Pneumocystis* exists in the cystic form, which has a thick-wall (approximately100nm) and reproduces sexually (6). In contrast, trophozoites have a thin wall that is approximately 20- 30nm, and are the most abundant in the host lung, and hypothesised to reproduce asexually via binary fission (5, 7). The most distinctive feature that distinguishes the cyst and troph are the macromolecules that make up the cell wall of these two forms (Figure 2). While the cystic form is composed mostly of β-glucans, which are easily recognised by the innate immune system, trophs lack these important glycoproteins (6, 8). The lack thereof is hypothesised to permit immune evasion by trophs (9). The cyst is the infective form, as cysts become airborne

allowing transmission between the infected and susceptible hosts. The infectivity of the cystic form was clearly demonstrated in a study where groups of rats were infected with *P. carinii* in either the trophozoite or cystic form. The rats infected with the trophozoites were unable to transfer infection to naive nude rats during cohabitation. However, rats inoculated with cysts were contagious, successfully transmitting infection to the naive athymic rats during cohousing (10).

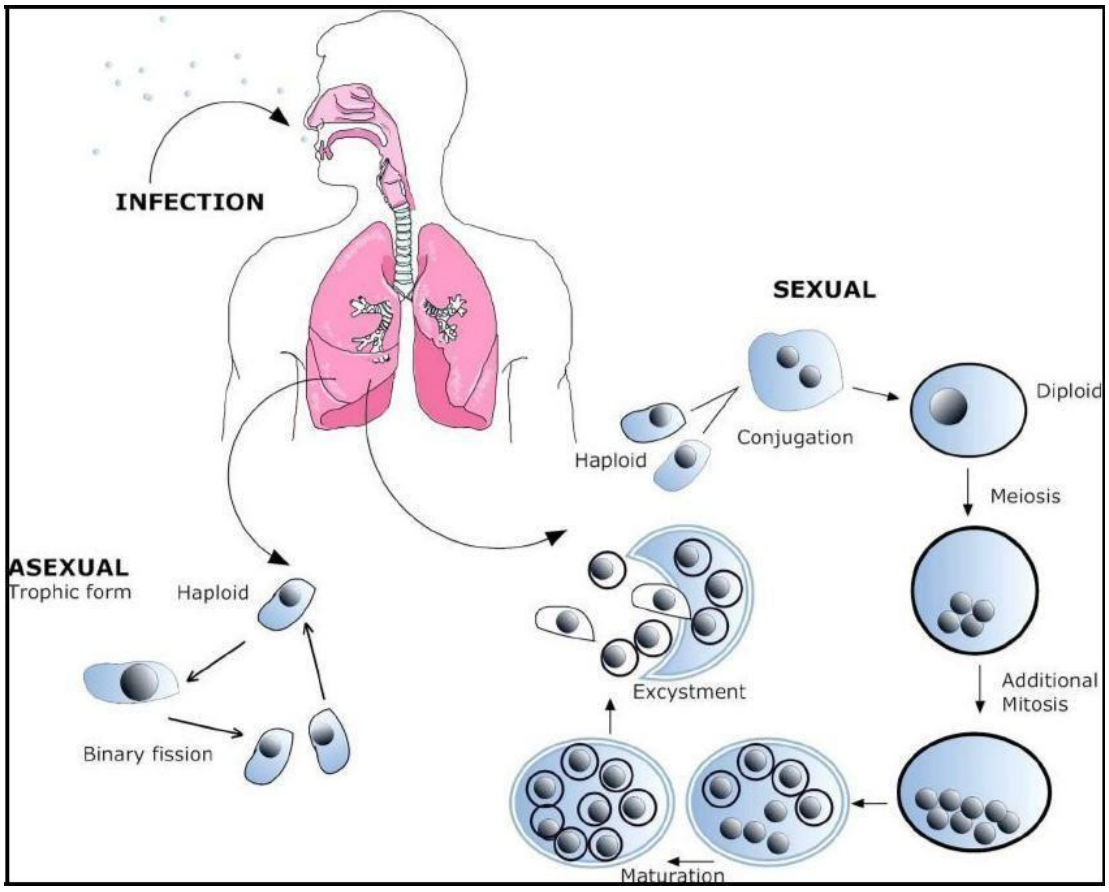

Figure 1: Proposed life cycle of *Pneumocystis*. Cyst and trophozoite are the two well-defined phases in the life cycle of *Pneumocystis*. The intermediate stage (depicted in the figure above) leading to mature cysts is known as the precystic phase, where 8 cysts are formed. Trophozoites predominate over cysts in the lung alveoli and are said to reproduce during acute infection through asexual reproduction. The cystic form is airborne and passes from host to host (11).

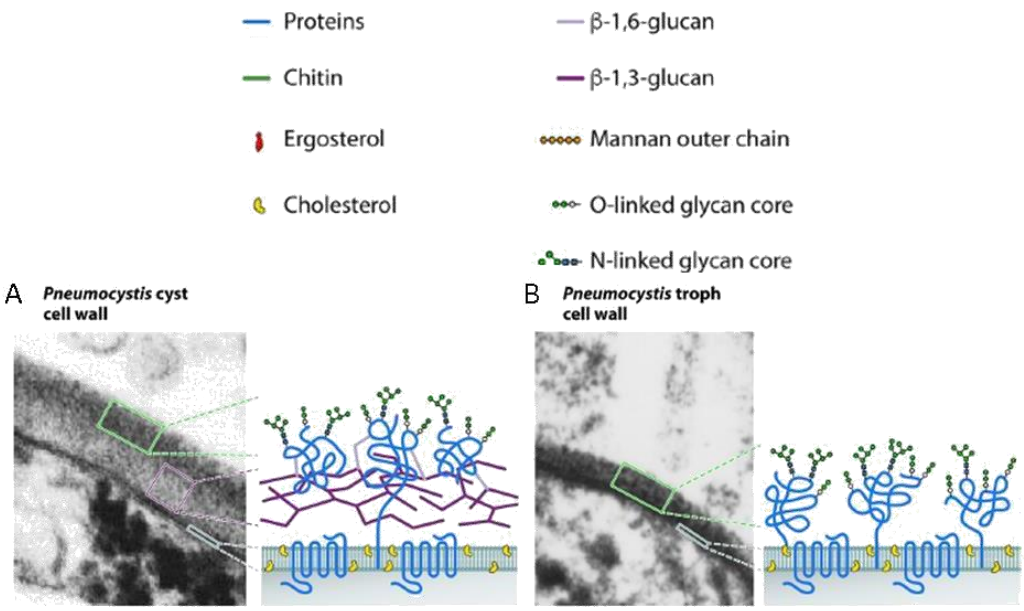

Figure 2: Cell wall components of Pneumocystis cyst and Pneumocystis troph. Both the cyst and the troph have N- and O- linked glycans outlying their cell wall A) The cyst's innermost layer is composed of β-glucans but lacks chitins. B) While the inner structure of the troph cell wall is composed of proteins and cholesterol but lacks both chitins and β-glucans. Adapted from (4)

1.2. *Pneumocystis* pneumonia

Fungal pneumonia, *Pneumocystis* pneumonia, emanates from failure of the immune system to control lung colonisation by *Pneumocystis* fungi. The global burden is estimated to be more than 200,000 of AIDS-related deaths, and more than a quarter of this is observed in non-AIDS-patients annually (12). In Sub-Saharan Africa the epidemiology is predominantly attributed to the high AIDS burden, as risk of infection is correlated with a significant decrease of $CD4^+$ T cells (13, 14). Furthermore, the high incidence rate reported in the European population and the United States are due to intervention therapies for other conditions that tamper with the functionality of the immune system such as autoimmune diseases, cancer and organ transplant (15, 16). A similar trend of a substantial increase in *Pneumocystis* cases recently observed in England is also attributed to underlying lung diseases (such as cystic fibrosis) and other forms of immune suppression excluding HIV (17).

1.2.1. Prevalence

Pneumocystis is among the greatest causes of opportunistic infections accountable for the high morbidity and mortality seen in immunocompromised individuals (18). Worldwide, *Pneumocystis* pneumonia is among the top ten of the most severe fungal infections affecting immunocompromised individuals (19). Prior to the 1980s *Pneumocystis* was known as the cause of pneumonia in premature, malnourished infants, as well as infants who suffered from a defective immune system (20, 21). In literature, we find evidence of the first cases of *Pneumocystis* dated back to the era of World War II in European orphanages. More *Pneumocystis* pneumonia cases were later reported in orphanages in Iran (22). As time progressed, new treatment strategies for other health conditions were introduced. These included the introduction of chemotherapy for cancer patients and immunosuppressive drug treatment for organ transplant patients. Although the therapies proved beneficial to the patients, as they limited the spread of cancer and prevented organ rejection, respectively, they also perpetuated the susceptibility of these patients to *Pneumocystis* pneumonia (23, 24). However, at that time there were only sporadic cases reported, until the outbreak of HIV/AIDS which introduced a new population of *Pneumocystis* pneumonia candidates (25). *Pneumocystis* pneumonia prevailed during the AIDS epidemic in the early 1980s with high incident rate among young homosexual men. Shortly after, *Pneumocystis* pneumonia was acknowledged as an AIDS defining-illness (22). Sub-Saharan Africa contributes 70% to the global HIV burden (14), however, this does not translate to the prevalence of *Pneumocystis* pneumonia in these countries. This is mainly due to the initiation of highly active antiretroviral therapy (HAART) which has had a great impact in reducing the high mortality rates precipitated by *Pneumocystis* in HIV-positive individuals (26).

1.2.2. Diagnosis and Treatment

The deleterious effect that *Pneumocystis* pneumonia has on the quality of health of immunocompromised individuals can be kept to a minimal through accurate diagnosis and timely treatment. The standard procedure is the staining of respiratory specimens, the bronchoalveolar lavage fluid (BAL) or induced sputum, using Grocott's staining technique and visualizing the cysts

or trophs under the microscope (27, 28). However, the disadvantage associated with this method is that accurate diagnosis is reliant on high *Pneumocystis* burden in the lung, consequently imperiling the development of severe hypoxia and lung damage in patient (29). Additionally, the extraction of BAL fluid or sputum induction, though proven to have a 98% sensitivity and accuracy, are very invasive procedures with high cost implications and require highly trained staff (30). Therefore, as a means to surmount the caveats that accompany the conventional diagnostic techniques real-time qualitative polymerase chain reaction (qPCR) was developed (31). This method showed the greatest efficacy for early detection as it could detect low levels of *Pneumocystis*, even before disease manifestation, whilst also reducing the chances of false-positive results (32, 33). New diagnostic techniques that are in the pipeline include the serum 1,3-β-D-glucan (BG) assay, which detects the cysts' innermost layer of the cell wall, 1,3-β-D-glucan, that is recognized by the host (34). Early and accurate diagnosis translates to early treatment and a reduced mortality rate.

Trimethoprim-sulfamethoxazole (TMP-SMX) is the first-line drug for the treatment of *Pneumocystis* pneumonia (25, 35). In HIV positive individuals, TMP-SMX treatment is administered as a preventative for *Pneumocystis* pneumonia development and is continued until the $CD4^+$ count increases to above 200 cells/μl (25, 36). Unfortunately, some patients experience an allergic response to the primary prophylaxis and are then given the secondary prophylaxis, Pentamidine (25, 29). In cases where an individual has had *Pneumocystis* pneumonia, they are given dapsone and atovaquone, which are secondary prophylaxis, to prevent reoccurrence (37, 38). Patients that experience mild to acute *Pneumocystis* pneumonia are treated with corticosteroids to alleviate chronic inflammation, consequently enhancing patient outcome (35). However, there are important limitations that cannot be overlooked concerning the invention of novel drugs for patients in constrained settings. These include, the route of drug administration, such as intravenous administration, which requires hospitalization, in areas that lack well equipped facilities and skilled staff to conduct the necessary treatment procedures. This has then prompted researchers to employ resources to investigate what

happens within the host, both those who control and clear the infection, and those in whom disease is exacerbated.

1.3. Immune system

The immune system is made up of organs, cells and molecules, collectively working together in the host mounting a defence against foreign invaders (39). The two arms of the immune system utilized against pathogens are the innate (natural) and adaptive (acquired) immune responses. The host uses these systems to distinguish between self and non-self-antigen, and to also recognise a previously encountered pathogen in order to mount a specific and a greater immune response (40, 41).

1.3.1. Innate immune response to *Pneumocystis*

Innate immunity is a very important component of the immune system as its primary role is to distinguish between self and non-self-antigens, consequently defending the host against invaders (40, 42). The principle of self and non-self-recognition is at the core of the innate immunity, and crucial for the immune system when deciding how to respond (43). Innate immunity is the immediate non-specific response mounted against an infectious pathogen (44). This system lacks immunological memory, therefore the response mounted is always to the same extent regardless of the number of times the same pathogen is encountered (39, 41).

The strategy employed by the innate immune system is that of pathogen associated molecular patterns (PAMPs) recognition. PAMPs are repeating conserved regions, unique for each group of pathogens that are essential for the pathogen to thrive within the host (45). These molecular patterns are then detected by pattern recognition receptors (PRRs) expressed by immune cells of the host (43, 46). Upon recognition, a release of chemokines and cytokines is triggered in an effort to eradicate the infection (47). The different types of PRRs utilized by the innate immune system include C-type lectin receptors (CLRs), Toll-like receptors (TLRs), NOD-like receptors (NLRs) and Retinoic acid-inducible gene (RIG)-I-like receptors (RLRs) (48). Of importance to this

study are CLRs, as they have been shown to play a crucial role in mediating innate immunity during fungal invasion (49).

CLRs are a group of receptors that effectively tailor antifungal innate immunity. These receptors recognise both endogenous and exogenous ligands via carbohydrate recognition domains (CRDs) thus initiating an immune response (Figure 3) (50). Furthermore, these CLRs can also bind non-carbohydrate ligands, such as lipids and proteins via C-type lectin-like domains (CTLDs) (49, 51). For example, Dectin-1 is a CLR characterised by a single CTLD and ushers a host protective immunity through the detection of β-glucans abundant on the cell wall of various fungi (52). Conversely, Dectin-2 and Mincle are classical CLR possessing a single CRD with a key role in fungal and bacterial recognition through various ligands on the surface of these pathogens (49, 53). Dectin-1, Mincle and Dectin-2 are all well-known Syk-coupled immunoreceptor tyrosine-based activation motif (ITAM)-bearing receptors with an important role in anti-fungal immunity. Their signalling mechanism is via the activation of the downstream molecule NF-κB through the Card9 pathway (Figure 3) (51, 54). The activation of this signalling pathway upon fungal recognition triggers proinflammatory cytokine production including IL-6, TNF, and IL-1β, and these cytokines have been established as key players in antifungal immunity (39, 55, 56). Other CLRs that induce intracellular signalling to confer anti-fungal immunity include DC-SIGN, Clecsf8 and the mannose receptor (MR) (55, 57, 58). Failure of these receptors to control infection triggers a compensatory mechanism which manifests through co-signalling.

Co-signalling is a phenomenon which requires the involvement of another PRR, such as a TLR or other CLRs, for robust response against pathogens. The cross talk between CLRs is an important component of innate immunity. Through these interactions these receptors regulate each other to mediate protective immunity. For example, Mincle, an important CLR that recognises both *Pneumocystis* and *Mtb* ligands is regulated by Clecsf8 (59, 60). Furthermore, Mincle-deficiency during *Pneumocystis* infection induces high expression of Dectin-1and Dectin-2 which translates into better survival of the mice as the disease progresses (60). In contrast, a first report on

downregulation of other CLRs during *P. murina* infection was demonstrated in Dectin-2-deficient mice (61). This, however, did not affect pathogen control in these mice. Overall, co-signalling of CLRs is an interesting mechanism that might be implicated in either enhanced or diminished immune response during *Pneumocystis* infection.

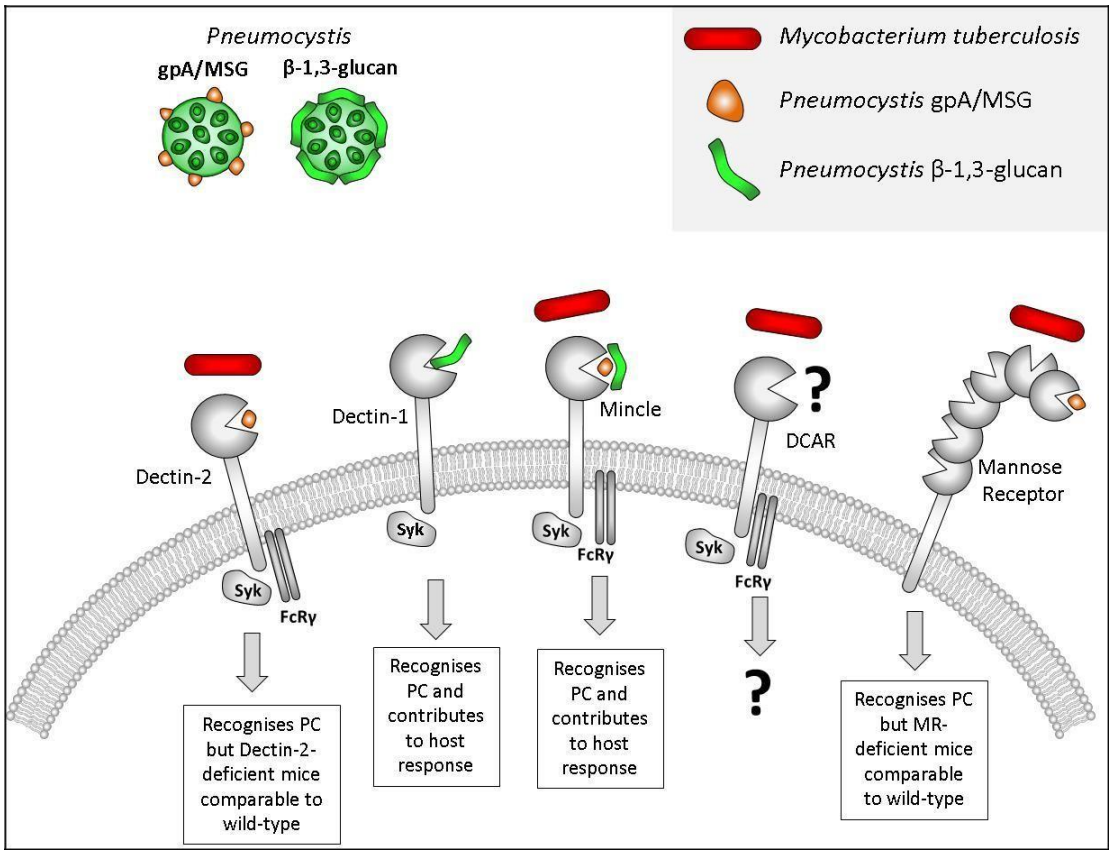

Figure 3: C-type lectin receptors that recognise both *Pneumocystis* and *Mycobacterium tuberculosis (Mtb)* ligands. Various ligands on the cell wall of both *Pneumocystis* and *Mtb* are recognised by their respective CLRs are shown in the figure above. Interestingly, no studies have shown recognition *of Pneumocystis* by DCAR, however, PIM is the ligand on the cell wall of *Mtb* shown to be recognised by this receptor. Adapted from (62, 63)

1.3.2. Adaptive immune response against *Pneumocystis*

In contrast to the innate immune responses, adaptive immune responses are specific and highly specialized. The response mounted is robust, much more sophisticated and specific to the antigen recognised. The adaptive immune response is highly driven by immunological memory which allows for quicker elimination of a pathogen that is reoccurring and confers longer lasting

protection (41). Adaptive immunity is afforded by two main groups of lymphocytes called B cells and T cells. The responses carried out by these lymphocytes include antibody responses and cell-mediated immune responses, respectively. When B cells encounter a foreign antigen bound to a major histocompatibility complex (MHC) presented by an APC, they secrete antibodies. In turn, these antibodies serve the function of coating the antigen, neutralizing and marking it for ingestion by phagocytic cells (41). B cells are also able to present to T cells by first internalizing and processing the antigen, and with the expression of an MHC complex and co-stimulatory molecules, activate T cells (62). Sequentially, T cells respond by either killing the pathogen directly, through killing the infected host cell, or send signals to other cells of the immune system (such as macrophages) for phagocytosis of the pathogen (39, 41).

$CD4^+$T cells are a major part of cell-mediated immunity against *Pneumocystis*. Hence, a decline in the number of $CD4^+$T cells leaves HIV positive patients vulnerable to infection (63). When $CD4^+$T cells are activated by an antigen they differentiate into subtypes including T helper type 1 (Th1), Th2, and Th17 effector T cells (64). These cells are characterised by their signature cytokines which perform unique effector functions during infection. Th1 cells primarily produce Interferon gamma (IFN-γ) as their signature cytokine, along with other pro-inflammatory cytokines (such as TNFα, TNFβ and IL-2). A Th1 response drives the production of IgG2a antibody, which confers protection against intracellular pathogens. Conversely, Th2 response signal against extracellular pathogens by producing interleukin 4 (IL-4), IL-5, IL-13, and IL-25, and promote the production of IgG1 and IgE antibodies (65). Studies have illustrated the importance of maintaining a balance between Th1 and Th2 responses during fungal infection, as excessive of either responses may have detrimental effects in the infected host (66). Another group of T cells, Th17 cells with a signature cytokine IL-17, were shown to play a compensatory role by enhancing the host immune response against pathogens (such as fungi and bacteria) when the Th1 and Th2 responses are not efficient at clearing the infection (67).

1.4. Dendritic cell immunoactivating receptor

C-type lectin receptors are the key players in early response against *Pneumocystis* infection. While inhibition of these receptors in mice promotes an increased fungal burden in the lungs, the mice eventually do clear the infection (61, 68). For example, Dectin-1- and Mincle-deficient mice present with high *Pneumocystis* burden and cannot efficiently produce cytokines, but the disease outcome is similar to that of wild type mice (19, 69). This implies that, although CLRs have an apparent role in controlling the fungal burden in the lung, clearance of the infection does not exclusively depend on CLRs, other PRRs and cells of the immune system are likely to be involved (61, 70). Other CLRs that have been shown to contribute to the resolution of fungal infections include Dectin-2 and DC-SIGN (49, 55).

The dendritic cell immunoactivating receptor (DCAR) is a new receptor, recently shown to function in *Mycobacterium tuberculosis* recognition (Figure 3) (71). DCAR is a type II CLR belonging to the dendritic cell immunoreceptor family (DCIR) (72). It is highly expressed by a distinguished subtype of DCs, antigen presenting cells and other myeloid cells (73, 74). A study by Kanazawa (2003) showed the various tissue sites at which this receptor is expressed, with the lung and spleen being the primary sites for this receptor, and low expression were observed in the skin and lymph nodes (75). Other CLRs that form part of the DCIR family include dendritic cell immunoinhibiting receptor (DCIR), Dectin-2 and blood DC antigen-2 (BDCA-2) (73, 76). DCAR and DCIR are said to be homologous due to similarities in their extracellular lectin domain, however, they possess different short cytoplasmic tails (75). DCAR bears an immunoreceptor tyrosine-based activating motif (ITAM), while DCIR is characterized by an inhibitory immunoreceptor tyrosine-based inhibitory motif (ITIM) (75, 77) . These receptors are expressed simultaneously on monocyte-derived inflammatory cells conferring a balanced signal at the surface of these cells. DCAR possesses a 82% amino acid sequence homology with Dectin-2, which is a classical CLR with a key role in antifungal immunity (72, 78). Of importance to note is that DCAR induces activating signals through its association with the FcR -γ chain, an association that has been noted to be crucial in other CLRs such as Mincle for protective immunity

during fungal infection (75, 79). In a tuberculosis (TB) mouse model of infection it was demonstrated that DCAR utilizes the Spleen tyrosine kinase (Syk)/Caspase recruitment domain family member 9 (CARD9) pathway to induce a Th1 immune response which is of priority during an active TB infection (71, 80). Interestingly, the role of this CLR has not yet been shown in *Pneumocystis* infection. Therefore, our aims were to determine disease progression in DCAR-deficient mice and analyse the early and adaptive immune responses that associate with the observed phenotype. We further wanted to assess the effect of cohousing experimental animals prior to experimentation.

Materials and Methods

Chapter 2. Materials and Methods

2.1. Mice

The following mice were used for experiments:

- Wild type (C57BL/6 background) (The Jackson Laboratory strain)
- *Clec4b1*$^{-/-}$ (C57BL/6 background) (71)

The mice were kept in individually ventilated cages (IVCs) under special pathogen free conditions at the Animal Unit facility located at the Chris Barnard Building, at University of Cape Town. The two strains of mice were cohoused in frequently cleaned cages with sufficient food and water supply. Only female mice were used for the purpose of this study, aged between 8-12 weeks. The mice were monitored daily for symptoms of adverse effects following infection and to ensure that they were not experiencing any distress or discomfort. The dendritic cell immunoactivating receptor (DCAR) knockout mice *(Clec4b1*$^{-/-}$*)* generated using Platinum TALEN (81) as previously described (82) were provided by our collaborators from Japan (Sho Yamasaki) and were kept at quarantine during the period of the study. This study was authorized by the UCT Faculty of Health Sciences Animal Ethics committee (015/046).

2.2. Genotyping

DNA extracted from DCAR$^{-/-}$ mice tail sections was used to confirm the genotype by polymerase chain reaction (PCR) analysis. To extract DNA, the mice tail clippings were incubated overnight at 56˚C in 500µl lysis buffer. After centrifugation at 10 000 rpm for 10 min, the supernatant was removed, and DNA was precipitated by isopropanol. After centrifugation at 10 000 rpm for 6 min, the pellet was washed with 70% ethanol and allowed to air dry. The DNA pellet was then resuspended in dH_2O and used for genotyping by PCR. A set of primers that were used in PCR to confirm *Clec4b1* gene deletion were purchased from the Department of Medical Biochemistry at the University of Cape Town.

The following primers were used for the purposes of genotyping DCAR$^{-/-}$ mice:

F: GGCTATCTCTGTGGTATTTAGCTC

R: CCCTACCTTGTAGCTGTCTT

The T100™ Thermal Cycler (BioRad) was used for PCR amplification of the *Clec4b1* gene using conditions set out in Table 1. $MgCl_2$, PCR buffer and Taq polymerase were purchased from Vector Laboratories (UK), and the dNTP stocks were obtained from Promega, Madison, United states.

Table 1: Amplification conditions for the *Clec4b1* gene

	Temperature ˚C	Time (seconds)
1. Initial denaturation	94	180
2. Denaturing	94	30
3. Primer annealing	60	30
4. Extension	68	30
5. Final extension	72	300
6. Repeat step	4	∞

Electrophoresis of the DNA from each sample was carried out on 1.6% agarose gels with 1x Tris borate ethylene di-amino tetra acetic acid (TBE) as the buffer. The gel was run at 180 Volts for 90 minutes and a 1 kb DNA ladder (Promega, Madison, United States) was used to determine the DNA size. The expected band size was 144bps, as was observed on the agarose gel (Figure 3.1).

2.3. Infection of mice with *Pneumocystis murina*

Pneumocystis cannot be cultured, therefore, Pneumocystis *was* propagated by infecting Rag-1-deficient mice with $5x10^5$ cysts in 100µl sterile LPS-free PBS (gibco by life technologies) via intratracheal instillation. Lungs were then harvested and kept in a -80 degrees Celsius freezer as stock. To prepare the inoculum, we isolated the cysts and trophs from infected RAG-1-deficient mouse lungs (stored at -80 °C) by mashing it through a 70µm sieve in 4ml of phosphate buffer saline (PBS). After centrifugation at 2000 rpm for 10 min, the supernatant was removed, and the pellet was resuspended in 1ml of PBS. To

count the cysts on a Fisher brand microscope slide we did a 1:10 dilution of the sample in PBS, and 5µl of the diluted sample was placed on the slide and left to air dry before staining. Diff-quick (Difco, Detroit, Mich) staining technique was used, which stains both cysts and trophs. After staining the sample, the slide was rinsed under running tap water and left to air dry before counting cysts under the x100 oil immersion lens of a light microscopy. To differentiate between cysts and trophozoites under a light microscope we identify the presence of one lucid nucleus, which is a phenotypic characteristic of trophozoites. While cysts are identified by the presence of multiple intracystic bodies (between 4 to 8 nuclei). To infect mice, we used a final concentration of $2x10^5$ cysts in 100µl of the inoculum, which we calculated using the following equation: πr where π=3.14 and r =No of cysts/2 and diluted with required volume of PBS. Both the control and experimental mice were co-housed for 2 weeks before infection, unless stated otherwise. On the day of infection, the mice were intraperitoneally injected with ketamine and xyalizine (80mg/kg and 16 mg/kg, respectively) for anaesthesia, then suspended vertically from their front incisors on suture wire. In order to gain access to the trachea and allow the mice to breath while anesthetised, the tongue was carefully extended to the left. Thereafter the mice were infected via intratracheal instillation with $2x10^5$ of the inoculum. Daily monitoring of mice was initiated post infection, until the pre-determined time points of sacrifice. Those involved in the study were accredited by the South African Veterinary Council for all animal experimental procedures.

2.4. Confirmation of death by cardiac puncture

At each sacrificial time point, halothane (5% in air) was used in an enclosed container to euthanize the mice. Mice were then placed dorsally on a board and 70% ethanol was sprayed to sterilize the area below the sternum before needle insertion. A 1ml insulin needle was inserted on a 20° angle just left of the xiphoid process. The syringe plunger was slowly retracted while gently moving the needle forward, and once the blood started flowing into the syringe, the needle was held steadily until blood 400µl to 600µl of blood was collected into a 600µl BD microtainer gel separation tube.

2.5. Collection of lungs

At the set time points following infection mice were sacrificed using halothane and cardiac puncture. They were then sterilized with 70% ethanol before opening them up. The ventral midsection was incised up to the neck region to remove the ventral skin. Another incision was made on the peritoneum from the lower abdomen towards the cervical region to expose the organs. The lungs were exposed by the cutting and removal of the rib cage. As the lung of a mouse is divided into five lobes, each lobe was aseptically collected into its respective collection tube. For histology purposes the left lobe was fixed in 4% formalin in PBS, the two right lobes were collected into 500µl of PBS + protease inhibitor for the tissue cytokine ELISA and bicinchoninic acid (BCA) assays, 800µl of trizol was used for collecting one lobe for RNA extraction, and the last lobe was removed and collected into 1ml of dulbecco modified eagle medium (DMEM) + 2% fetal bovine serum (FBS) for flow cytometry. All samples were immediately homogenised and stored at -80, excluding the flow cytometry samples which were processed, stained, fixed on the day of the kill and acquired within 7 days.

2.6. Quantification of *Pneumocystis*

RNA extraction

Lung samples collected in Trizol which were homogenized and stored at -80 °C were thawed at room temperature (RT). Using chloroform each sample was separated into phases of DNA, protein and RNA by centrifugation at 12 000 rpm for 10 min. The top aqueous layer was transferred into separate 2ml eppendorf tube and isopropanol was used for RNA precipitation. The pellet was then washed in 1ml 75% ethanol following centrifugation for 10 min. The pellet was left to dry before adding 50µl of dH_2O, and the RNA concentration and purity were read on the Nanodrop ND-1000 Spectrophotometer prior to making cDNA.

cDNA synthesis

All our RNA samples were normalized to 1µg per reaction to compensate for contaminating mouse RNA present in the samples. From each sample 1µg of RNA was converted to cDNA using the iScript cDNA synthesis kit from Bio-Rad, as per the manufacturer's instructions. The kit contains 5X iScript reaction mix, iScript Reverse Transcriptase and Nuclease-free water. The required volume of each reagent was added, and DNA was synthesized using the following conditions:

Table 2: cDNA synthesis conditions

	Temperature ˚C	Time (minutes)
1. Priming	25	5
2. Reverse transcription	46	20
3. Reverse Transcription incubation	95	1

qPCR

To quantify *Pneumocystis* the small subunit rRNA gene of *P. murina* was targeted using specific primers (described below). The starting concentration of our arbitary standard was 10^8 copies and a series of 10-fold dilution were performed with the lowest standard at 10^{-3}copies. The SsoAdvanced quantitative RT-PCR (qRT-PCR) universal probes master mix was prepared as detailed in the Table 3 below. In a 96 well PCR plate we added 15µl of the Master mix followed by 5µl of the cDNA and covered with a clear PCR plate seal before centrifuging the plate at 1200 rpm for 1min. After centrifugation the reaction was ran on the Real time PCR machine.

SSU primer and probe sequences are as follows: Forward 5'-CATTCCGAGAACGCAATCCT-3'; Reverse 5'-TCGGACTTGGATCTTTGCTTCCCA-3'; FAM-Probe: 5'-TCATGACCCTTATGGAGTGGGCTACA-3'

Table 3: PCR Master Mix ingredients and volumes

PCR Master Mix	Volume (µl)
2x Supermix	10µl
40x Primer mix	0.5µl
H_2O	4.5µl

2.7. Flow cytometry

Immediately after the collection of lungs on sacrificial day the lungs were cut into small pieces and then incubated at 37°C for 90 min in digestion buffer (Appendix A). After incubation the lungs were minced through a 70µm cell strainer before centrifugation at 1500 rpm for 10 min. The precipitate of cells was then removed, and the red blood cells were lysed using Red blood cell lysis buffer (RBC) (Appendix A) at room temperature for 1 min after which 5ml of PBS was added to stop the reaction. Subsequently, FACS buffer (Appendix A) was used for resuspension of cells after the second wash with PBS. Trypan blue was then used to stain 20µl from each sample and the cells were counted with a haemocytometer under a light microscopy. The remaining cells were then stained with 25µl of lineage-specific cell-surface markers (table 4) and incubated in the dark for 30 min on ice. FACS buffer was then added to stop the staining process after which the cells were fixed before filtering and acquiring on a FACS LSRII (Beckton Dickinson) flow cytometer using FACS Diva version 6.0 (Beckton Dickinson). All samples were analysed using Flowjo V10 software (Treestar, USA).

Table 4: Flow cytometry Antibodies

Antibody	Clone name	Source
Antigen presenting cells markers		
APC Rat Anti-Mouse Ly6G	1A8	BD Pharmingen
Alexa Fluor® 700 Hamster Anti-Mouse CD11c	HL3	BD Pharmingen
V450 Rat Anti-Mouse CD11b	M1/70	BD Horizon
APC-Cy 7™ Rat Anti-Mouse Siglec f	E50-2440	BD Pharmingen
Rat mAb to Neutrophil (7/4) (FITC)	GR288279-11	Abcam
BV510 Rat Anti-Mouse CD45	30-F11	BD Horizon
PE/Cy7 Anti-Mouse F4/80	BM8	Biolegend
T cell markers		
BV421 Hamster Anti-Mouse CD3e	145-2C11	BD Horizon
PE Rat Anti-Mouse CD44	IM7	BD Horizon
FITC Rat Anti-Mouse CD8a	53-6.7	BD Horizon
Alexa Fluor® 700 Rat Anti-Mouse CD4	RM4-5	BD Horizon

2.8. Enzyme linked immunosobernt assay

Cytokine production levels in lung tissue were measured using an ELISA kit as per manufacturer's instructions (BD OptEIA). Cytokines of interest that were measured include, TNF, IL-1, IFN-γ, IL-12p70, IL-12p40, IL-6, and IL-10. Briefly, 96 Maxisorb Nunc (Nalge Nunc International, Naperville, IL, USA) well plates were coated with 100µl/well of Capture antibody diluted in coating buffer (Appendix A) and left to incubate at 4°C overnight. The plates were then washed 3 times with washing buffer (Appendix A) and blocked with blocking buffer (Appendix A) 200µl/well and incubated at RT° for 1 hour. While the plates were incubating, the recombinant standard was prepared according to

the manufacturer's instructions (starting concentration Table5). After incubation period was completed, the plates were washed 3 times, and100µl of the recombinant standard was added to appropriate wells in 2-fold serial dilutions. Samples were also added, and the plates were incubated at RT° for 2 hours. The plates were again washed with a total of 5 washes and the Detection antibody + Enzyme reagent (Streptavidin-horseradish peroxidase conjugate) were diluted in Assay diluent and 100µl/well was added to each plate and incubated at RT° for 1 hour. At the end of incubation, the washing step was repeated with a total of 7 washes, and 100µl/well of PNP substrate solution (4-nitrophenyl disodium salt-hexahydrate) (1mg/ml in Substrate Buffer, Appendix A) was added and plates were developed at RT° in the dark. Thereafter, 50µl/well of sulfuric acid was added to stop the reaction and the absorbance was read at 450nm within 30 min of stopping the reaction using a VERSA max Tunable Microplate Reader (Molecular Devices Corporation, California, United States) and data analysis was achieved using Soft Max Pro Version 4.3 Software (Molecular Devices Corporation, California, United States).

Table 5: Cytokine ELISA kit Antibody dilutions/ Recombinant concentration

Cytokine	Capture Antibody	Detection Antibody	Enzyme Reagent	Standard Concentration	Source
TNFα	1:250	1:1000	1:250	4ng/ml	BD Biosciences
IFN-γ	1:250	1:250	1:250	2ng/ml	BD Biosciences
IL-1β	1:250	1:500	1:250	2ng/ml	BD Biosciences
IL-12p40	1:250	1:1000	1:250	1ng/ml	BD Biosciences
IL-12p70	1:250	1:250	1:250	4ng/ml	BD Biosciences
IL-6	1:250	1:500	1:250	1ng/ml	BD Biosciences

2.9. Histology

Lung samples collected in 10% Formalin from mice at pre-determined time points were sent to the laboratory at the Department of Surgery, Groote Schuur Hospital. A qualified technician sectioned and embedded the lung sections in wax. The process includes dehydration and rehydration, as detailed in Table 6 and 7 below.

Table 6: Dehydration

	Number of changes	Length of procedure
70% Alcohol	1	30 minutes
96% Alcohol	2	45 minutes
100% Alcohol	4	45 minutes
Xylol	2	60 minutes
Wax (55°C to 60°C)	2	45 minutes

The lung samples were embedded in wax and then trimmed into thin sections. The thin tissue sections were then floated in a warm water bath after which the sections were placed onto glass slides and incubated at 37°C for 2-18 hours to remove the wax. Tissue rehydration process for staining is shown below in Table7.

Table 7: Rehydration

	Number of changes	Length of procedure
Xylol	1	3 minutes
Xylol	2	1 minute
Absolute Alcohol	2	1 minute
96% Alcohol	2	1 minute
70% Alcohol	1	1 minute
Water	1	1 minute

The rehydrated tissue was stained with either the Grocott's Methenamine silver stain (GMS) (used to stain fungal organisms), or Periodic acid–Schiff (PAS), or Haematoxylin and eosin stain (H&E). Photomicrographs were captured using Nikon DS-Ri2 high performance camera and analysed with the NIS Elements AR 4.30.01 imaging software.

2.10. Statistics

Statistical comparison between two groups was performed using student's t-test, with a two-tailed distribution, unless stated otherwise. All statistical analysis was completed using Graph Pad Prism (version 6) and data is demonstrated as the mean ± SEM. For all tests, a p-value< 0.05 was considered statistically significant.

Results

Chapter 3. Results

3.1. Confirmation of Dendritic Cell Immunoactivating Receptor (DCAR) deletion in mice

DCAR-deficient mice were genotyped to confirm the deletion efficiency of the *Clec4b1* gene (Figure 3.1). This was done by digesting tail sections from mice and extracting DNA for PCR analysis. The expected band size was 144bps, as was observed on the agarose gel (Figure 3.1). Lanes 2 to 10 showed bands of 144bp, which were the expected band sizes from mice with DCAR deficiency. DNA extracted from WT mice served as a positive control and showed a band size of 150bp (lane 11). We added H_2O to the PCR reaction as a negative control (lanes 12 &13) and no bands were observed.

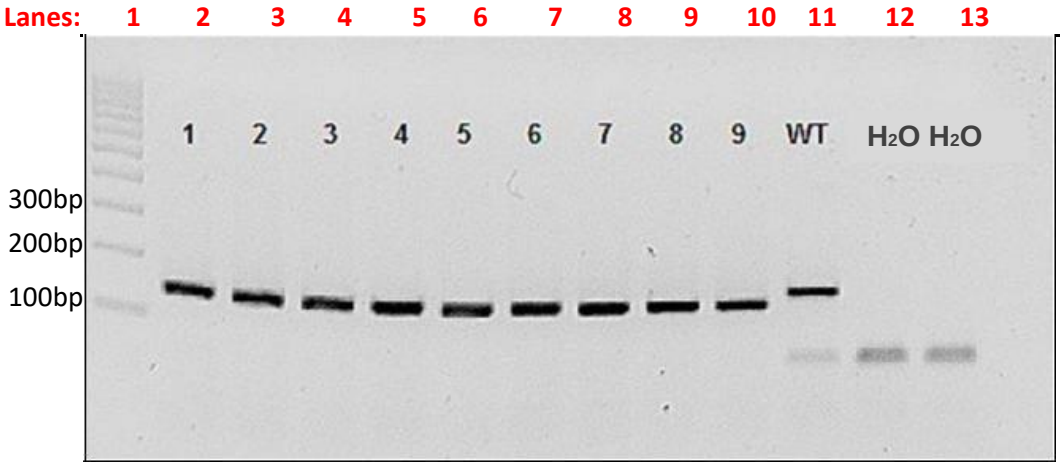

Figure 3. 1: Genotyping of DCAR-deficient mice. DNA extracted from $DCAR^{-/-}$ mouse tails was amplified by PCR and ran on electrophoresis agarose gel to visualise the band size. Lanes 2 to10 show bands at 144bp which represents $DCAR^{-/-}$ mice. Lane 11 shows a band at 150bp, which is the expected size for WT mice which served as our positive control. Lanes 12 and 13 show no bands as water was used as a negative control

3.2. *Pneumocystis murina* standard

Pneumocystis species are not viable in culture. Therefore, to quantify the fungal burden we established a qRT-PCR assay. Under the guidance of Georgia Schäfer, we made a standard using a plasmid (pGEM-T-SSRNA1.1) containing the mitochondrial RNA (mtRNA) insert of *P. murina* sent to us by Jay Kolls (USA). The pGEM-T-SSRNA1.1 spotted on filter was transformed into *Escherichia coli* (*E. coli*) TOP10 cells. Colonies were then selected for sequencing. After digesting 4ug of pGEM-T-SSRNA1.1 with the restriction enzyme Not I for release of the insert, the product was then run on a 1% agarose/TAE gel to check for complete digestion with a 3kb band size expected (Figure 3.2 A). After purification of the linearized plasmid, a final concentration of 168ng/ul was achieved. An amount of 1.5ug of the linearized plasmid was used for *In Vitro* Transcription (IVT). The product was then run on 1.5% agarose/MOPS gel to control for a single product and confirm the size of the IVT product (Figure 3.2 B).

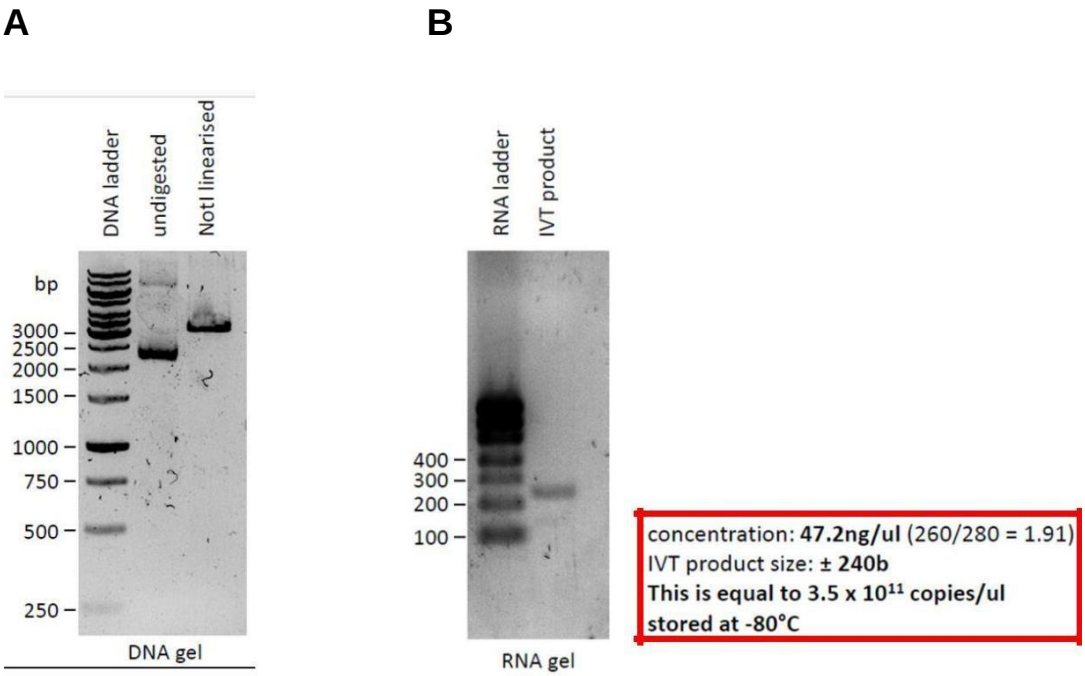

Figure 3. 2: *Pneumocystis murina* standard. *Pneumocystis* quantification by qPCR requires a standard of known concentration. Therefore, a plasmid containing *P. murina* mtRNA was transfected into *E. coli* bacteria. A) After complete digestion of the plasmid, linearization was confirmed on an agarose gel. B) The IVT product was transcribed into RNA, run on a gel, and the IVT product was stored at -80 C at a concentration of 47.2ng/ul.

3.3. DCAR deletion enhances *P. murina* clearance

CLRs have an important role in *Pneumocystis* recognition, potentially contributing to clearance (60, 69). Previously, Dectin-1, a phagocytic cell specific CLR, has been shown to facilitate protective immunity during *Pneumocystis* infection (69). Therefore, we sought to investigate the role of DCAR, a newly described dendritic cell receptor, during *P. murina* infection. To carry out this experiment, both the experimental and control mice were co-housed for 2 weeks prior to infecting them with $2x10^5$ *P. murina* organisms. Lungs were harvested at pre-determined time points and various immune parameters were measured to assess disease progression and pathology. Using qPCR, we were able to detect and quantify *P. murina* in the lungs of infected mice. Shown in Figure 3.3A is a graphical representation of *P. murina* quantification, where we observed reduced fungal burden in $DCAR^{-/-}$ mice in comparison to WT mice, at both day 7 and day 14 post-infection. We further used Grocott's methenamine silver (GMS) staining to visualise *P. murina* cysts in mouse lung tissue. Although GMS stain only detects the cysts and not the trophic form of *P. murina,* the microscopy visualisation showed similar fungal burden as the PCR quantification, with $DCAR^{-/-}$ mice exhibiting a lower *P. murina* burden compared to WT mice (Figure 3.3B). Both mouse strains had cleared the infection by day 21 post-infection (Figure 3.3A&B). Figure 3.3C shows representative GMS stained histology pictures taken from WT lung tissue samples at 40X magnification for clear visuals of clusters of cysts.

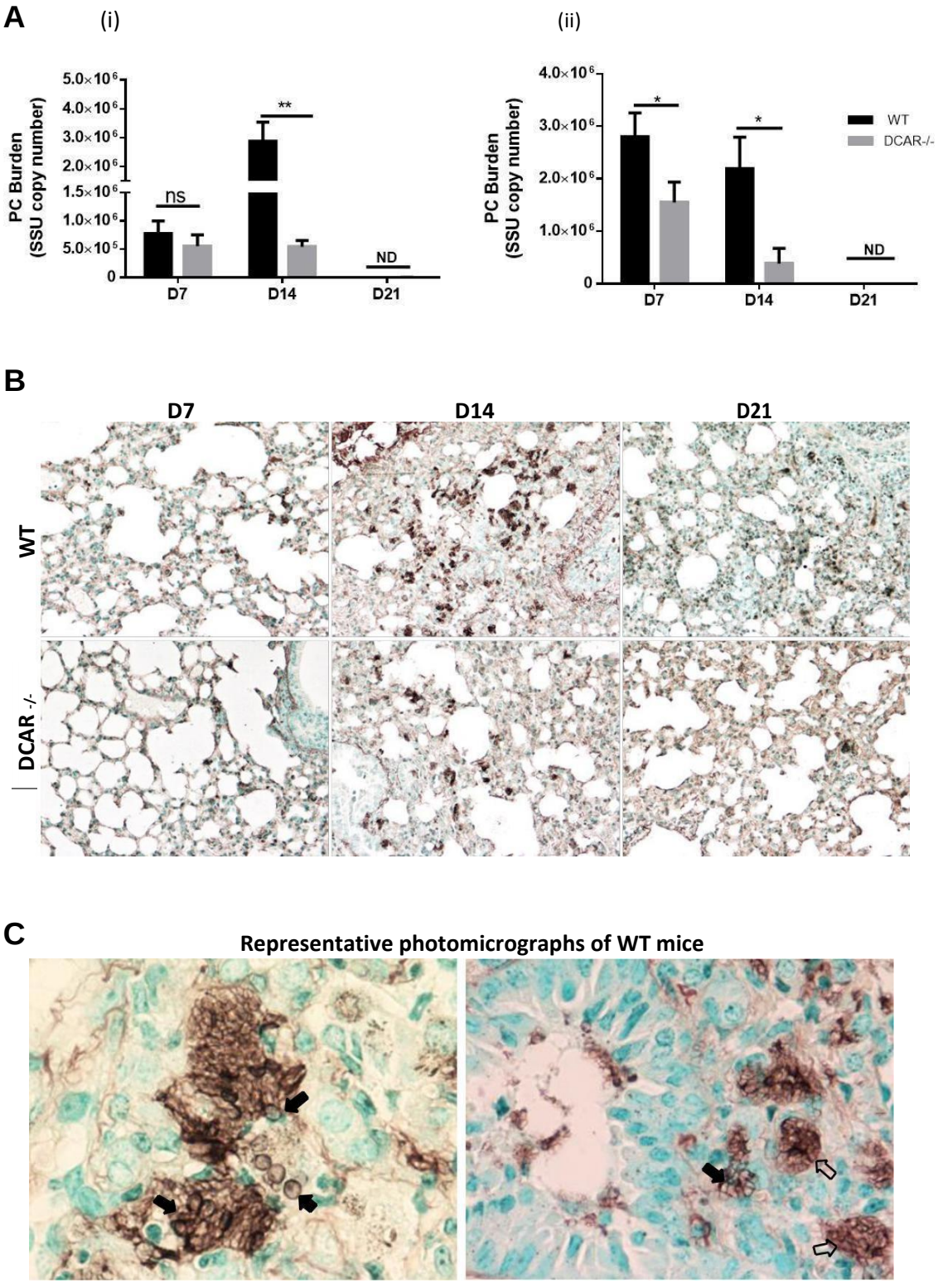

Figure 3. 3: *Pneumocystis murina* burden quantification and visualisation in DCAR-/- and WT mice. A) *P. murina* was quantified using qRT-PCR at the pre-determined timepoints (i & ii are two independent repeat experiments). B) Representative photomicrographs of *P. murina* in lung tissue stained with GMS (20X magnification). C) WT representative pictures taken 40X magnification (single cysts and clusters of cysts indicated by solid black arrows and open black arrows, respectively). The results shown indicate the mean ±SEM of five mice per group for all time points. Significant differences (* $p<0.05$, ** $p<0.01$) were determined using the unpaired one-tailed and two-tailed student's t tests for figure 3.3 A (i) and (ii) respectively.

3.4. Localisation of Inflammatory cells

Lung samples that were collected in 10% formalin were sectioned and embedded onto slides for histopathology analysis. Tissue samples were then stained with Haematoxylin and eosin (H&E) stain, which stains nucleated cells with a dark purple colour, to assess the localisation of cells in the lungs of *P. murina* infected mice. At day 7 there were no apparent differences between the DCAR$^{-/-}$ and WT mice. By day 14 there was seemingly greater cell infiltrates into the lungs of DCAR$^{-/-}$ mice compared to WT mice (Figure 3.4&B), however, when we quantified free alveolar spaces, the percentage difference was comparable between DCAR$^{-/-}$ and WT mice (Figure 3.4C). A greater accumulation of inflammatory cells was observed around the peribronchiolar regions of DCAR-deficient mice 14 days post-infection. When looking at a later time point, we noted that an influx of cells was still pronounced at day 21 in DCAR$^{-/-}$ mice, which had subsided in WT mice (Figure 3.4A&B). Furthermore, cells were markedly dispersed on the alveolar regions of DCAR$^{-/-}$ mice 21 days post-infection compared to WT mice, whose alveolar spaces were clear of cell infiltrates. To confirm our observations of the microscopic analysis, we further quantified free alveolar spaces and these results validated the histologic analysis (Figure 3.4C).

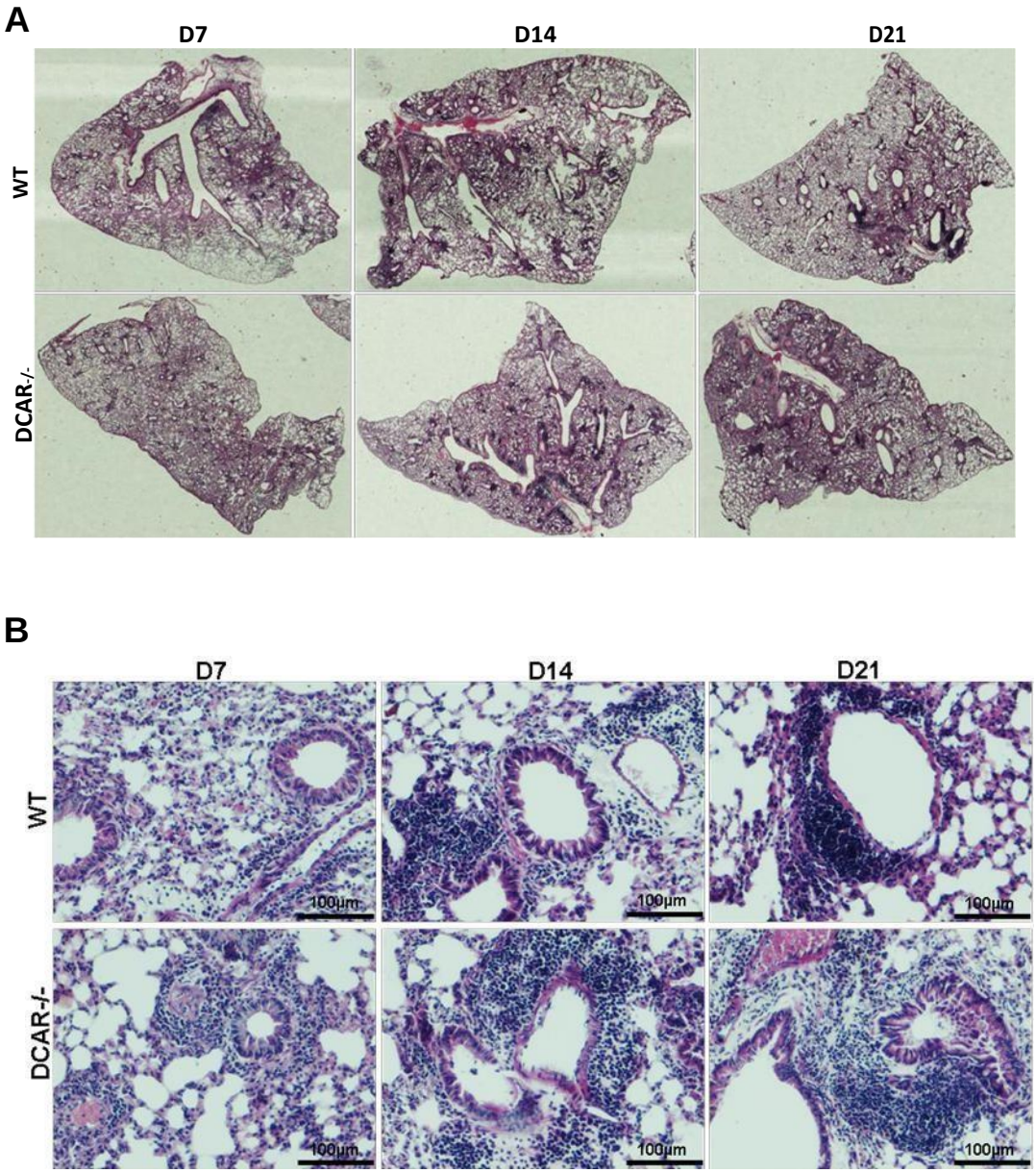

Figure 3. 4: Determining cellular infiltration by H&E staining. Mice infected with $2x10^5$ *P. murina* were euthanized at D7, 14 & 21. A) H&E stained photomicrographs showing an overview of lung tissue cross-sections (4X magnification). B) Lung sections magnified at 20X for clear representation of cell. C) Representative graph of quantification of free alveolar spaces represented as percentages. An unpaired two-tailed student's t test was done.

3.5 Cellular response during *P. murina* infection

To assess the immune cells that were recruited during *P. murina* infection, mice were euthanised and lungs harvested and processed (outlined in materials and methods) for FACS analysis. After single cell suspensions were prepared, samples were stained with the following antibodies:

Myeloid cell panel: Ly6G (APC), CD11c (Alexa Fluor 700), CD11b (V450), Siglec-F (APC-Cy 7), 7/4 (FITC), CD45 (BV510), F4/80 (PE/Cy7) (Figure 3.5A).

T cell panel: CD3 (BV421), CD4 (Alexa Fluor 700), CD8 (FITC), CD44 (PE/Cy7) (Figure 3.5B)

Samples were acquired using a flow cytometer and analysed by FlowJo software. Single cells were gated on to rule out doublet populations and AMs were identified as Siglecf^{+} F4/80^{+}. Markers used for DCs were CD11c^{+}Siglecf $^{-}$7/4^{-}, inflammatory monocytes were identified as CD11b^{+} 7/4^{+}, neutrophils were identified as Ly6G^{+}CD11C^{-}, and eosinophils were marked as Siglecf^{+}7/4^{-}.

Alveolar macrophages in conjunction with other immune cells, such as DCs and neutrophils, form part of the host's immediate response during *P. murina* infection (3). Therefore, the observed reduced fungal burden in DCAR$^{-/-}$ mice (Figure 3.3) propelled us to determine cells that were involved in the initial host response post-infection. We observed an increase in AMs along with DCs in DCAR$^{-/-}$ mice at day 7 compared to WT mice (Figure 3.6A). There was also a trend towards an increase in neutrophils in DCAR$^{-/-}$ mice, however this increase was not statistically significant (Figure 3.6A). Interestingly, although detected in low levels 7 days post-infection, eosinophils and inflammatory monocytes showed an increased trend in DCAR$^{-/-}$ mice at day 7. At day 14 a trend of higher cellular infiltration in DCAR$^{-/-}$ mice was maintained, however, these observations were not statistically significant. A similar trend observed in the total number of cells translated to the percentage representation of our myeloid cells of interest, with a significant decrease in AMs, DCs and inflammatory monocytes at day 21 in DCAR-deficient mice (Figure 3.6B).

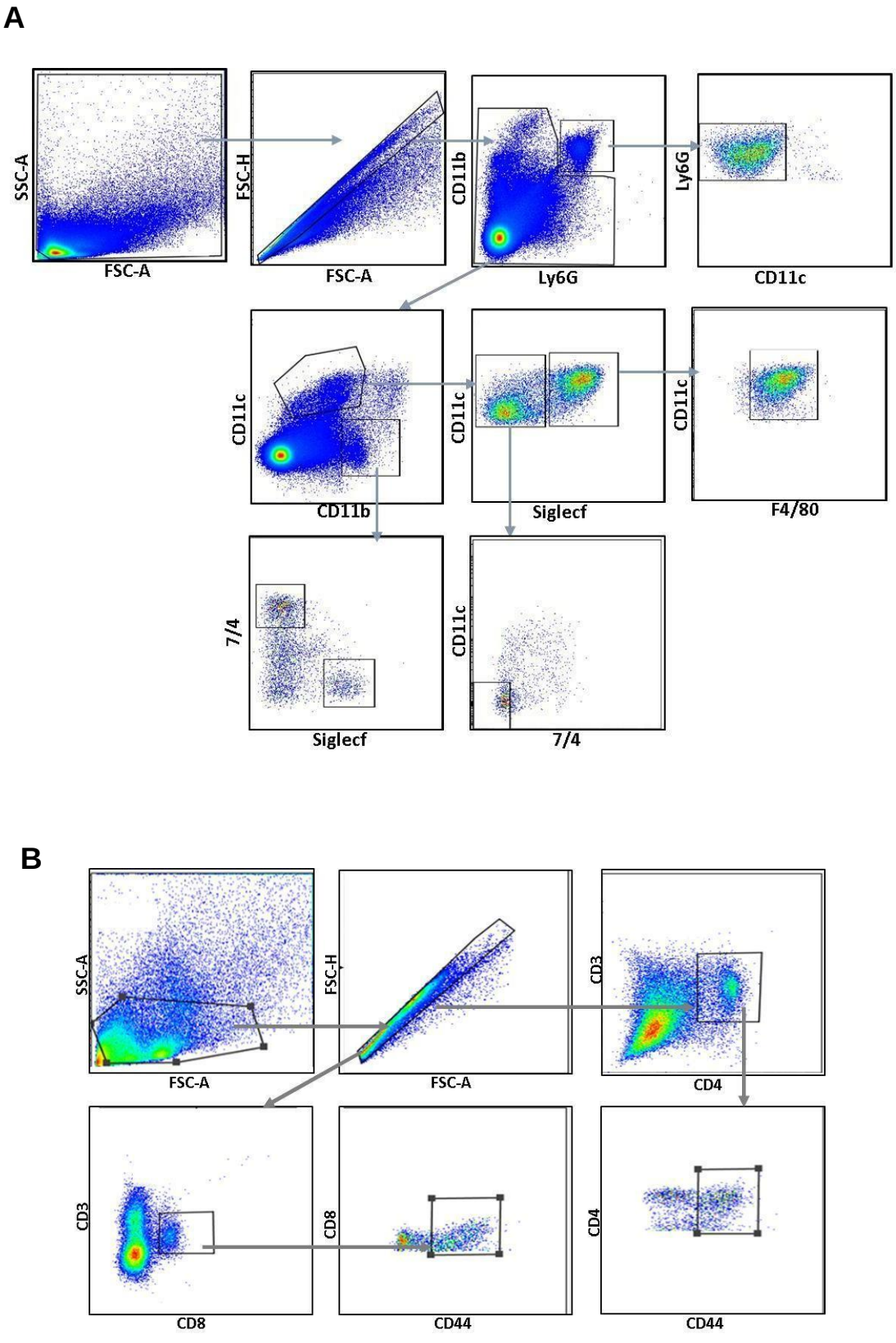

Figure 3. 5: Gating strategy for myeloid cells and lymphocytes. Lung cells from WT and DCAR$^{-/-}$ mice were isolated and labelled accordingly. A) By gating from the myeloid population, we identified: AMs (Siglecf^{+}F4/80^{+}), DCs (CD11c^{+}Siglecf^{-}7/4^{-}), neutrophils (Ly6G^{+}CD11c^{-}), Inflammatory monocytes (CD11b^{+}7/4^{+}) and eosinophils (Siglecf^{+}7/4^{-}). B) T cells were characterised as either activated CD4 T cells or CD8 T cells (CD3^{+} CD44^{+}).

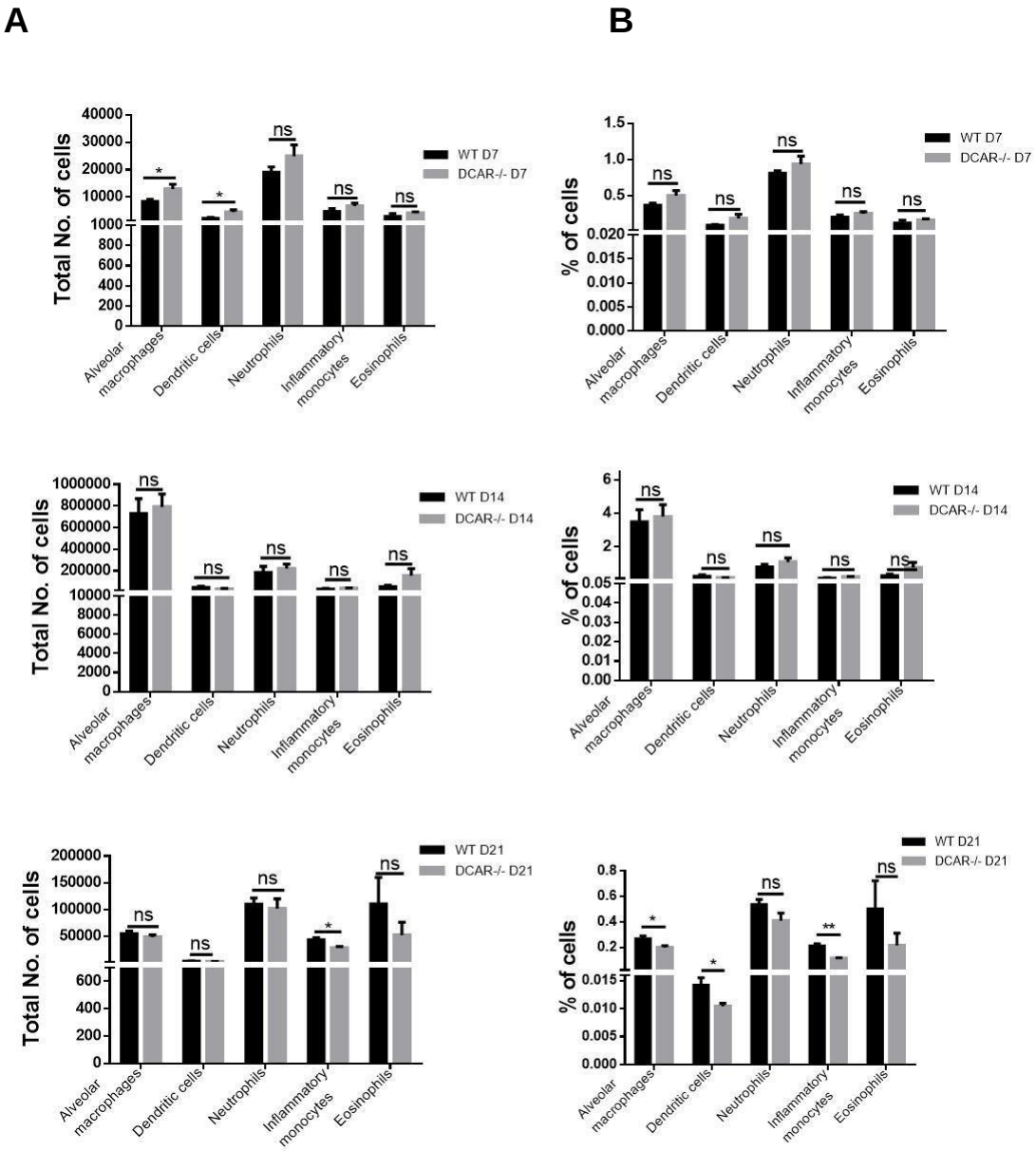

Figure 3. 6: Cellular responses post *P. murina* infection was measured by flow cytometry. WT and DCAR$^{-/-}$ mice were infected with 2x10^5 of *P. murina* and sacrificed at the indicated timepoints. The graphs show a comparison between absolute numbers and percentages. A&B) Cellular responses in the lungs of both WT and DCAR$^{-/-}$ were measured overtime. The results are expressed as mean ± SEM (n = 5 mice/strain per time point). Significant differences (* $p<0.05$, ** $p<0.01$) were determined using the unpaired one student's t-tests. Data shown are representative of two individual repeat experiments.

3.6. T cell recruitment during *P. murina* infection

T cells, specifically $CD4^+$ T cells, are crucial in protection against *Pneumocystis* infection. Several studies have shown host susceptibility to *Pneumocystis* infection to be rendered by a depletion of these cells (63, 83). We therefore analysed T cell recruitment during *Pneumocystis* infection in mice. As early as day 7 post-infection we saw increased $CD4^+$ T cells recruitment, as well as activated $CD4^+$ T cells ($CD4^+CD44^+$ T cells) in the lungs of $DCAR^{-/-}$ mice (Figure 3.7A). Additionally, we observed high number of $CD8^+$ T cells and activated $CD8^+$ T cells ($CD8^+CD44^+$ T cells) in DCAR-deficient mice (Figure 3.7A). By day 14 the number of T cells that were recruited into the lungs were still increased in $DCAR^{-/-}$ mice compared to WT mice, with notable statistical differences (Figure 3.7A). Looking at the frequency of T cell responses, we saw no significant differences at day 7 in both mouse strains (Figure 3.7B). However,14 days post-infection a significant increase was observed in the percentage of all T cell subsets in $DCAR^{-/-}$ mice (Figure 3.7B). By day 21 T cell responses were comparable between DCAR-deficient and WT mice (Figure 3.7A&B).

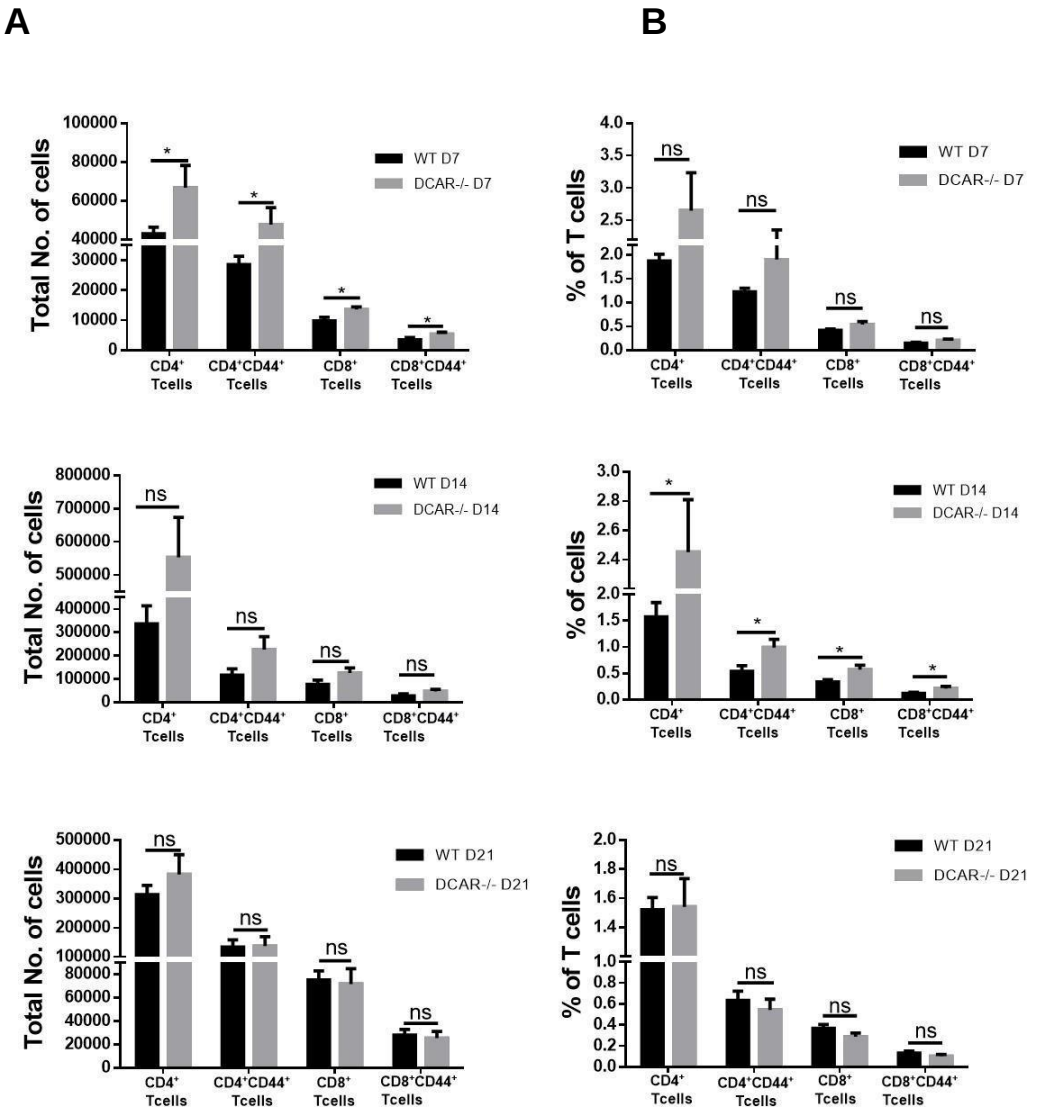

Figure 3. 7: T cell recruitment post *P. murina* infection was measured by flow cytometry. WT and DCAR$^{-/-}$ mice were infected with 2x10^5 of *P. murina* and sacrificed at the indicated timepoints. A) T cell recruitment in both WT and DCAR$^{-/-}$ mice was determined overtime. B) The percentage representations of T cells that were recruited during infection. The results are expressed as mean ± SEM (n = 5 mice/strain per time point). Significant differences (* $p<0.05$) were determined using the unpaired one-tailed student's t- tests. Data shown are representative of two individual repeat experiments.

3.7. Cytokine production post *P. murina* infection

Myeloid cells such as alveolar macrophages induce the production of specific cytokines for their effective function. Some of the key cytokines that have been implicated in enhancing immune response during *P. murina* infection include TNFα and IFN-γ (84). Other proinflammatory cytokines evidently play a contributory role in *Pneumocystis* clearance, include IL-1β, IL-6 and IL-12. We therefore sought to determine the cytokine profile exhibited by mice over the course of infection. Interestingly, although DCAR$^{-/-}$ mice showed a trend towards an increase in TNFα, IL-1β and IL-6 production as early as day 7, these differences were not statistically significant (Figure 3.8A). There were no differences noted in the production of IL-12p40 from both WT and DCAR$^{-/-}$mice throughout the experimental time points. The production of IL-10, an anti-inflammatory cytokine, was significantly impaired in DCAR$^{-/-}$ mice 7 days post-infection, and this trend persisted throughout to the last experimental time point (day 21) (Figure 3.8A).

A

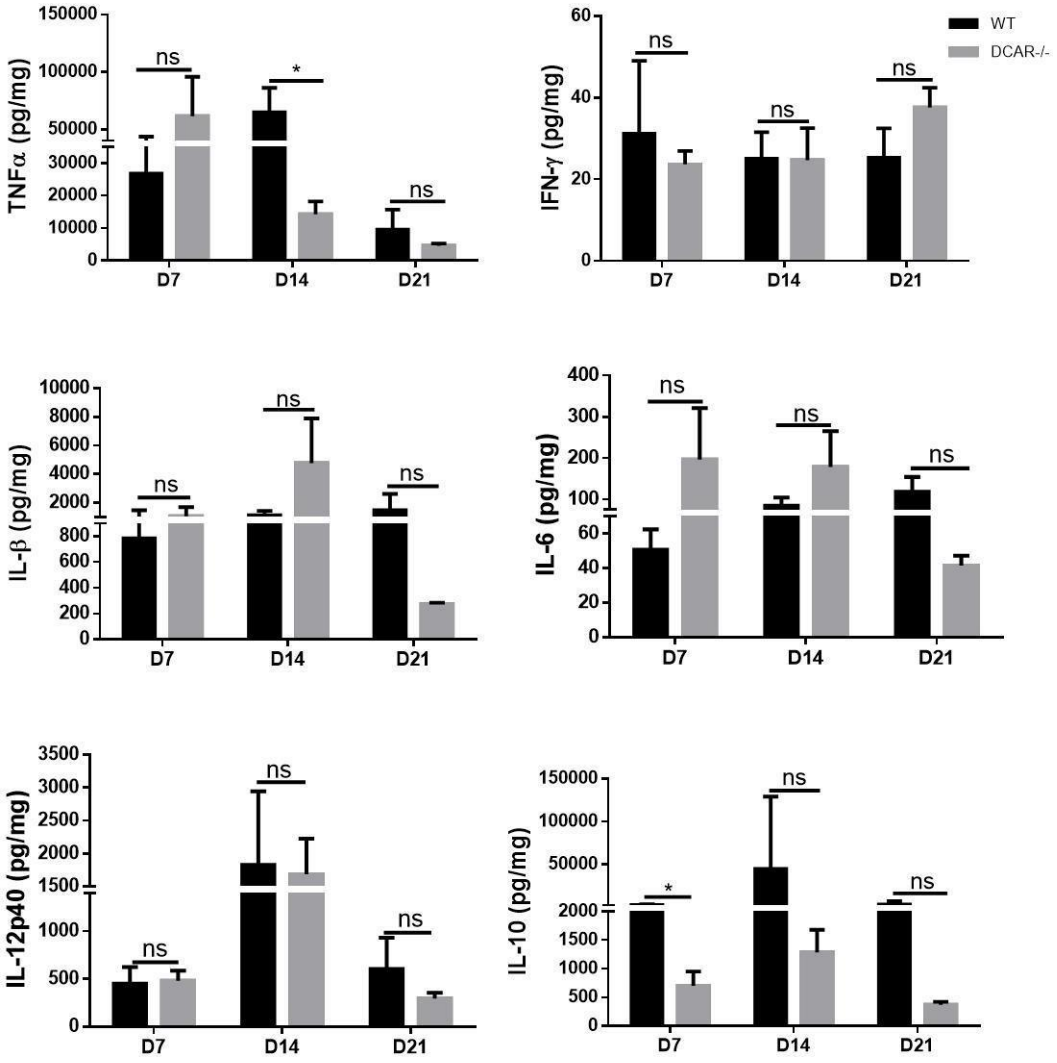

Figure 3. 8: Cytokine production from lung homogenates measured by ELISA assay. Mice were infected intratracheally with $2x10^5$/100µl of *P. murina* and cytokine levels were detected at D7, D14, & D21. A) Cytokine production determined in WT and $DCAR^{-/-}$ mice. The results are expressed as mean ± SEM (n = 5 mice/strain per time point). Significant differences (* $p<0.05$) were determined using the unpaired one-tailed student's t- tests. Data shown represent one individual experiment.

3.8. Assessment of Mucus production

Periodic acid–Schiff (PAS) stain, which detects polysaccharides and mucosubstances, was used to determine mucus secretion from hypertrophic goblet cells. Goblet cells secrete mucus as a means of clearing lung infection, and therefore would not be present in uninfected mice. In contrast, excessive mucus production can lead to lung tissue damage. In our study we found that DCAR$^{-/-}$ mice secreted mucus at all time points compared to WT mice, which only had pronounced production at day 14 (Figure 3.9A). Mucus production was sustained in DCAR$^{-/-}$ mice which had waned in WT mice (Figure 3.9A). These pictures are representative and for an accurate assessment of mucus production, quantification would be required.

A

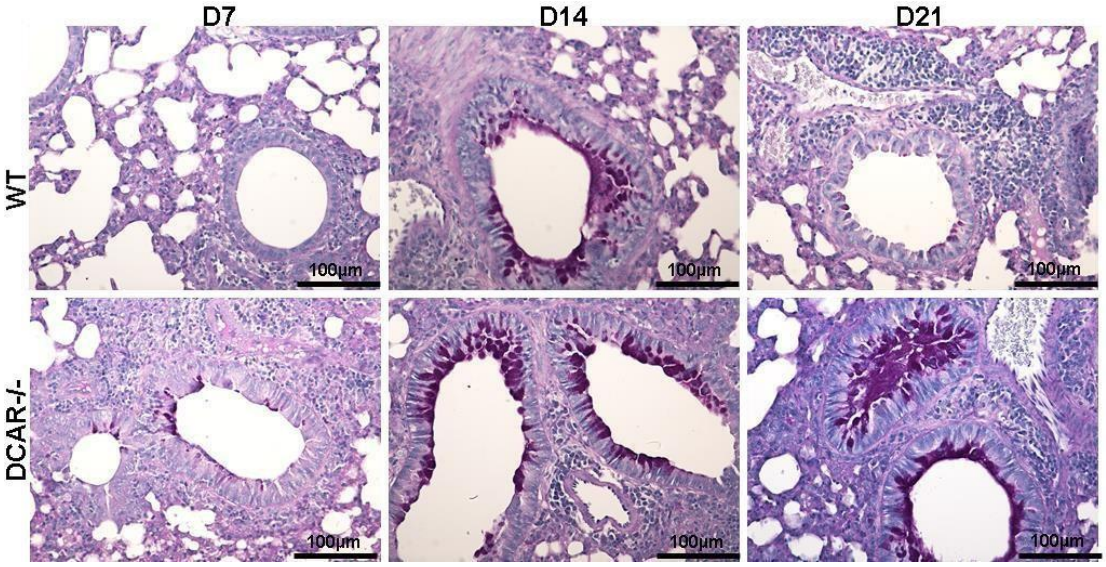

Figure 3. 9: Detection of mucus production in lung tissue. Mice infected with 2x10^5 *P. murina* were euthanized at indicated time points. C) PAS stain was used to assess mucin expression (an indication for mucus production). Histology pictures were taken at 20X magnification and are representative of two repeat experiments

3.9. Immune response 48 hrs post *P. murina* infection

Based on our observation of reduced *P. murina* burden at day 7 in DCAR$^{-/-}$mice, we wanted to further investigate whether there was a robust early response. We therefore, infected both DCAR$^{-/-}$ and WT mice with 2x10^5 *P. murina* organisms via intratracheal instillation and our control mice were treated with PBS only. At 48 hours post-infection mice were sacrificed, and BAL fluid was collected to analyse cell infiltration by flow cytometry and cytokine production by ELISA. There were no significant differences in the total number of cells between DCAR$^{-/-}$ and WT mice that were treated with PBS (Figure 3.10A), suggesting a comparable homeostatic state before infection of these mice. Following infection, there were also no significant differences in the number of myeloid cells in DCAR-deficient compared to WT mice (Figure 3.10A). However, the percentage difference of AMs and DCs was significantly high in PBS treated DCAR$^{-/-}$ mice when compared to *P. murina* infected DCAR$^{-/-}$ mice, with no apparent differences in other cell types (Figure 3.10B).

We further analysed cytokine profile exhibited by these mice 48 hours post-infection. Interestingly, we observed a significant increase in IL-6 production, as well as a trend of increased IFN-γ and IL-12p40 levels in PBS treated WT mice. Furthermore, there was notably a significant increase in IL-1β levels in DCAR$^{-/-}$ PBS treated mice compared to WT mice (Figure 3.11A).

Overall these data show that the DCAR deletion enhances *P. murina* clearance in mice. This ability is characterised by an early AMs and DCs response, which in turn trigger an adaptive immune response. Both CD4$^+$ and CD8$^+$ T cells are recruited to the site of infection to carry out their effector function throughout the course of infection. Thus, DCAR deficiency enhanced inflammatory responses critical for early *P. murina* clearance. However, whether these result in hypoxia or lung injury, as suggested by the seemingly low percentage of free alveolar spaces and excessive mucus production in DCAR-deficient mice, remains to be determined.

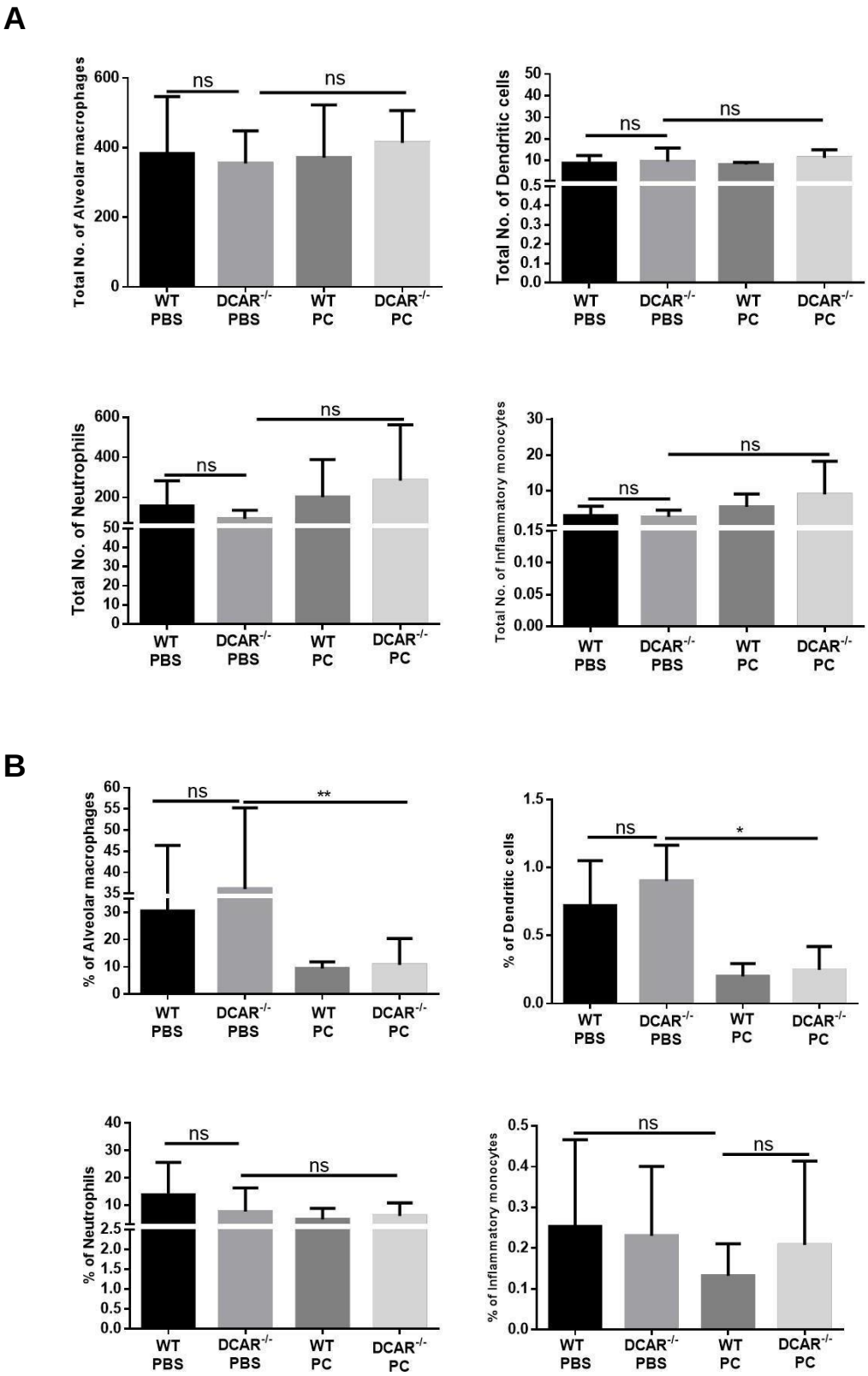

Figure 3. 10: Early response in mice at 48 hrs post-infection. BAL was collected from mice that were either infected with $2x10^5$ of *P. murina* or treated with PBS. (i) Innate cell responses measured by flow cytometry. (ii) Percentages of cells that were recruited to the lungs. Results are expressed as mean ± SEM (n = 6 mice/strain per time point). Significant differences (* $p<0.05$, ** $p<0.01$) were determined using the unpaired one-tailed student's t- tests. Data shown represents one individual experiment

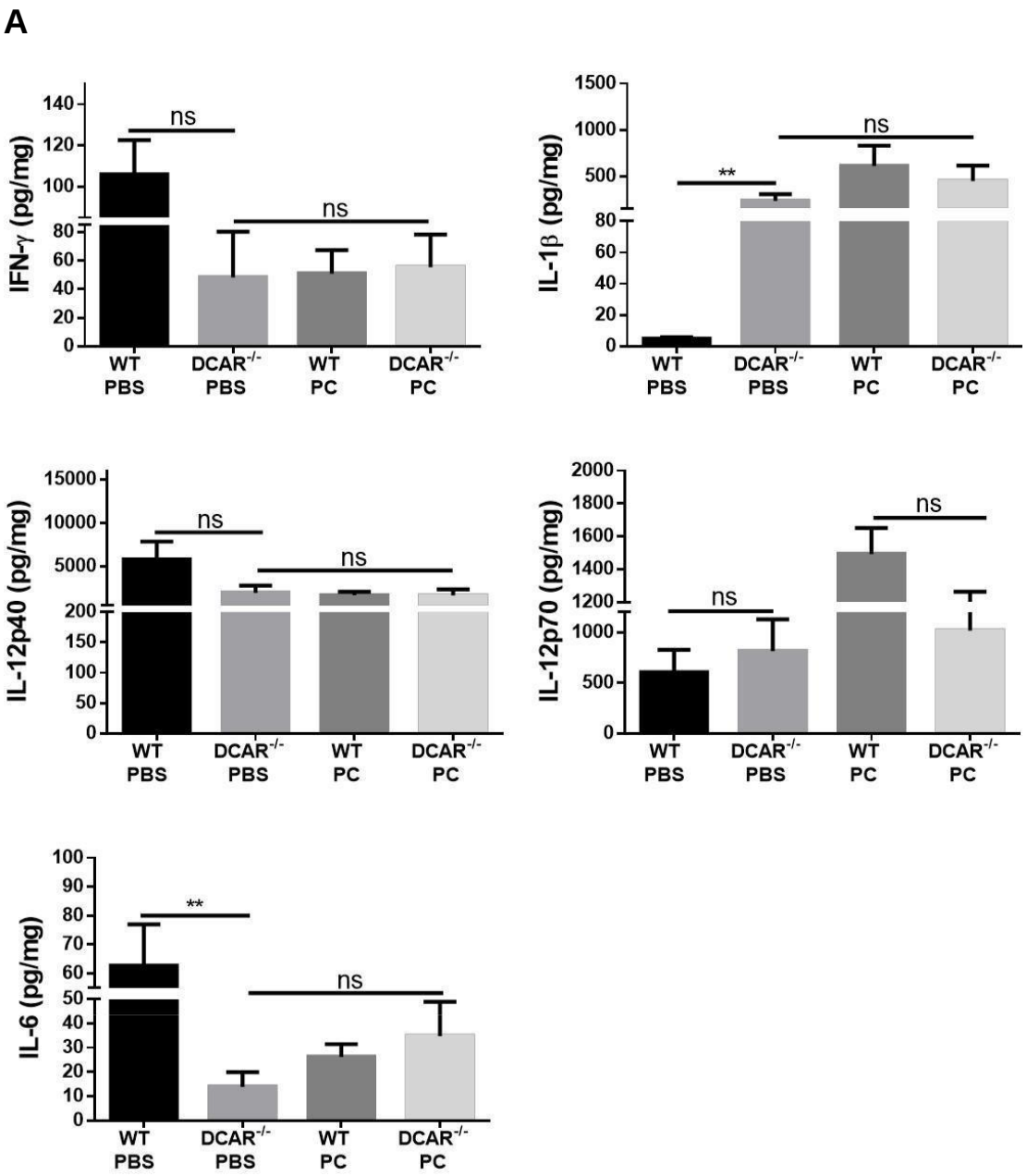

Figure 3. 11: Cytokines produced by WT and DCAR-/- mice at 48 hrs post infection. BAL was collected from mice that were either infected with $2x10^5$ of *P. murina* or treated with PBS. A) Cytokine production was measured by an ELISA assay. The results are expressed as mean ± SEM (n = 5 mice/strain per time point). Significant differences (**p<0.01) were determined using the unpaired two-tailed student's t-tests. Data shown represents one individual experiment.

3.10. The effect of co-housing in mice

Host microbiome plays an important role in influencing the immune response mounted during pathogenic invasion (85). Moreover, the environment as well as diet are essential determinants of the host's microbial composition (86). A passive transfer of microbiota between hosts occurs during co-housing. In our initial experiments we observed variability in our results and sought to determine the source of this variability. Therefore, cohabitation was introduced as means to rule out any external factors that may be of influence on the phenotype observed. We compared fungal load in co-housed and non-co-housed mice. For co-housing purposes, mice were delivered to the experimental facility, biosafety level 2 (BSL2), and marked by ear clippings. Thereafter, mice were randomly mixed, while ensuring that each cage had both DCAR$^{-/-}$ and WT mice. The mice were then kept together for at least 2 weeks before infection. Conversely, the non-housed mice were delivered to BSL2 and left to acclimatize for at least 2 days before infecting them with *P. murina*. Subsequently after infection with *P. murina* via intratracheal instillation, mice were sacrificed at the pre-determined timepoints (indicated in the graphs below). When the *P. murina* lung burden were quantified by qPCR, a significantly higher fungal burden 7 days post-infection in co-housed WT mice was observed (Figure 3.12A). However, WT mice that were not co-housed prior to infection showed a lower fungal burden (Figure 3.12B).

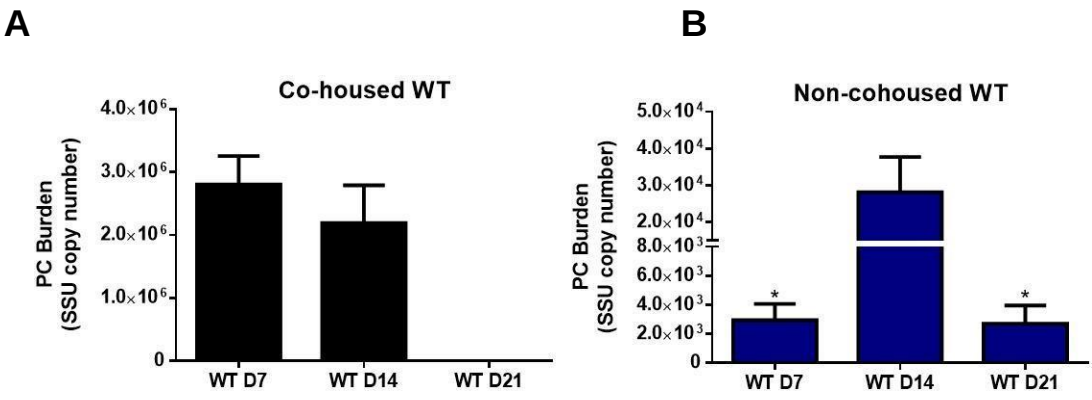

Figure 3. 12: *Pneumocystis murina* burden measured in co-housed and non-co-housed WT mice. *P. murina* burden was quantified by qPCR at D7, D14, and D21. A) Fungal burden in co-housed mice. B) Fungal burden in non-co-housed mice. The results shown indicate the mean ± SEM of the values of five mice per time point in each group. Significant differences for both figure 3.12 A and B were determined using the unpaired two-tailed and one-tailed student's t- tests (*p<0.05), respectively, comparing both D7 and D21 against D14. Figure3.12 A is also included in Figure 3.3A.

3.11. Early cellular immune responses in co-housed vs non-co-housed WT mice

Upon the observed differences in fungal burden in co-housed and non-co-housed mice, we then wanted to determine if there were differences in immune cell response in the two settings. As depicted in the results, at 7 days post-infection the co-housed WT mice had increased alveolar macrophages, neutrophils, and inflammatory monocytes (Figure 3.13A). These cells gradually decreased over time, except the alveolar macrophages which were again upregulated by day 21. Conversely, non-co-housed WT mice showed stunted alveolar macrophage and dendritic cell recruitment at day 7 (Figure 3.13 B), however, these cells peaked by day 14 and were again reduced by day 21. Neutrophils showed an increased trend at day 7, and inflammatory monocytes were significantly higher at day 7 and gradually decreased over time (Figure 3.13B).

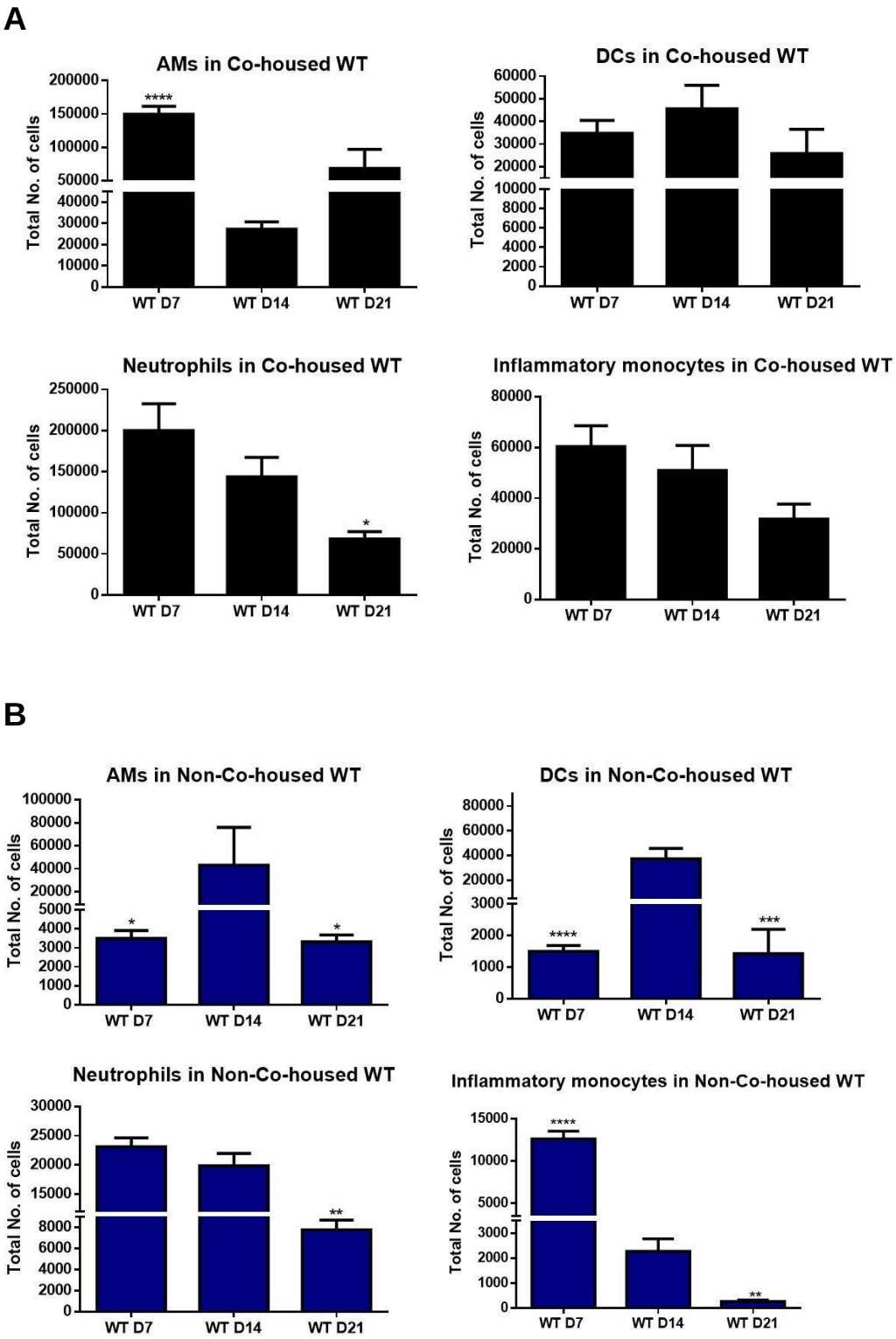

Figure 3. 13: Early responses post *P. murina* infection in co-housed vs non-co-housed WT mice. WT mice were infected with $2x10^5$ of *P. murina* and sacrificed at D7,14 &21. A) Cellular responses in co-housed WT mice. B) Cellular responses in non-co-housed WT mice. The results are expressed as mean ± SEM (n = 5 mice per time point). Significant differences were determined using the unpaired two-tailed student's t- tests (*p<0.05, **p<0.01, ***p<0.001, ****p<0.0001) comparing both D7 and D21 against D14. Data shown represents one individual experiment. Figure 3.13A is also included in figure 3.5A.

3.12. T cell recruitment in co-housed vs non-co-housed mice

We further investigated if the differences observed in innate responses would translate into variabilities in adaptive immunity. T cell recruitment was low in co-housed WT mice 7 days post-infection, except for the activated $CD4^+$ T cells which remained constantly high throughout the course of infection (Figure 3.14A). $CD8^+$ T cell recruitment peaked at day 14 and was reduced by day 21 (Figure 3.14A). Additionally, $CD4^+$ T cells were significantly increased at day 21 in co-housed WT mice. In contrast, non-co-housed WT mice maintained a trend of a significantly lower T cells recruitment 7 days post-infection, which increased by day 14 and were reduced significantly by day 21 (Figure 3.14B).

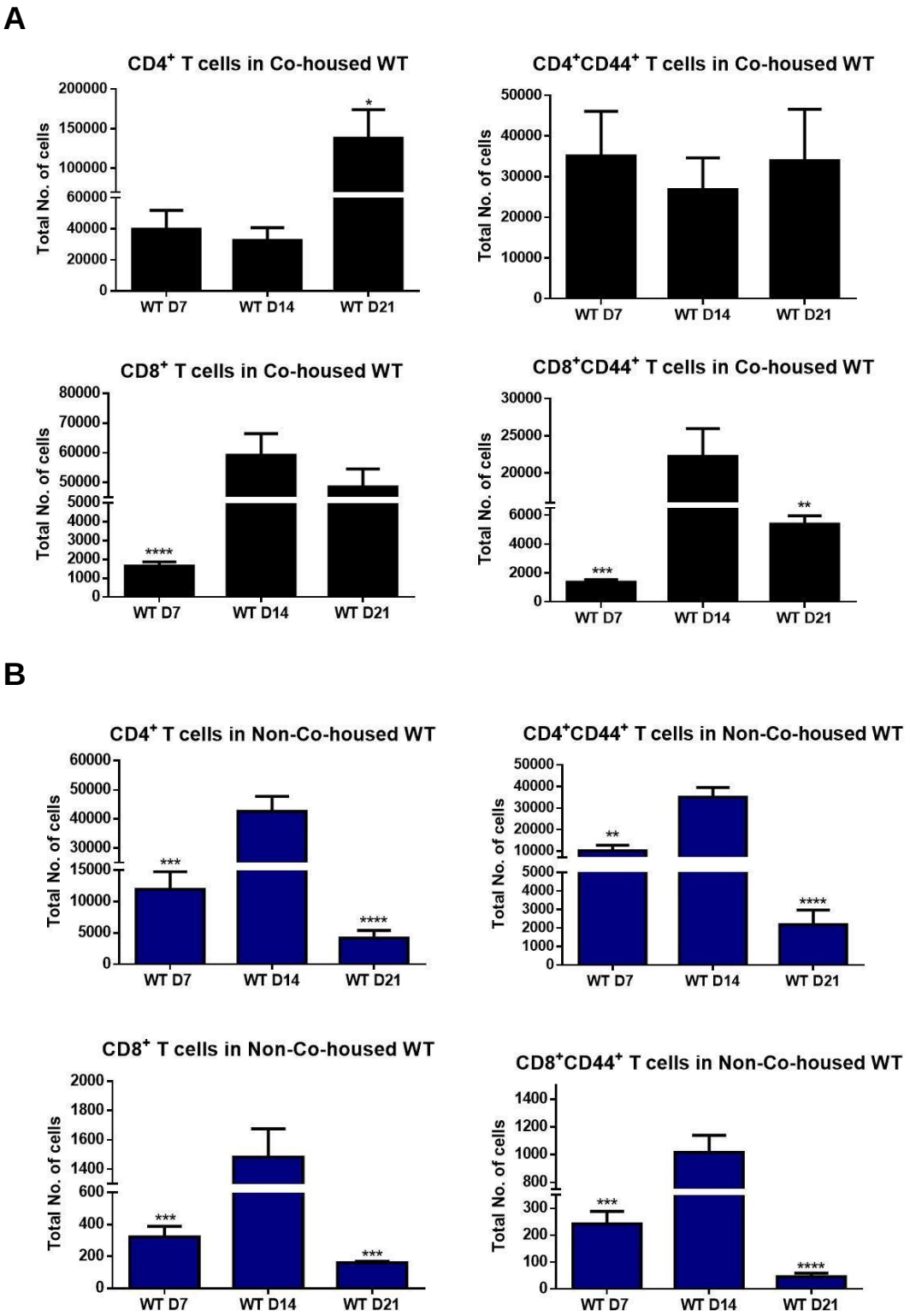

Figure 3. 14: T cell recruitment post *P. murina* infection in co-housed vs non-cohoused WT mice. WT mice were infected with $2x10^5$ of *P. murina* and sacrificed at D7, 14 & 21. A) Cellular responses in co-housed WT mice. B) Cellular responses in non-co-housed WT mice. The results are expressed as mean ± SEM (n = 5 mice/strain per time point). Significant differences were determined using the unpaired two-tailed student's t- tests (*p<0.05, **p<0.01, ***p<0.001, ****p<0.0001) comparing both D7 and D21 against D14. Data shown represents one individual experiment. Figure3.14 A is also included in figure 3.7A.

3.13. Cytokine production in co-housed vs non-co-housed mice

To further investigate the differences in immune responses in mice that were co-housed and those that were not co-housed we analysed their cytokine profiles by an ELISA assay. The differences observed in immune cell responses led us to deduce that there would be differences in cytokine production in mice that were in the two settings. Overall the cytokine pattern was similar between co-housed verses non-co-housed mice (Figure 3.15A&B). This included the production of IFN-γ, IL-1β and IL-6. Although the level of IL-1β production was low in the co-housed mice at day 7, it gradually increased over time (Figure 3.15A). While the pattern of TNFα production was quite similar for both groups at D7 and D14 (Figure 3.15A&B), co-housed mice presented with significantly reduced TNFα at day 21(Figure 3.15A). TNFα remained elevated in non-co-housed mice until the last experimental time point (day 21) (Figure 3.15B).

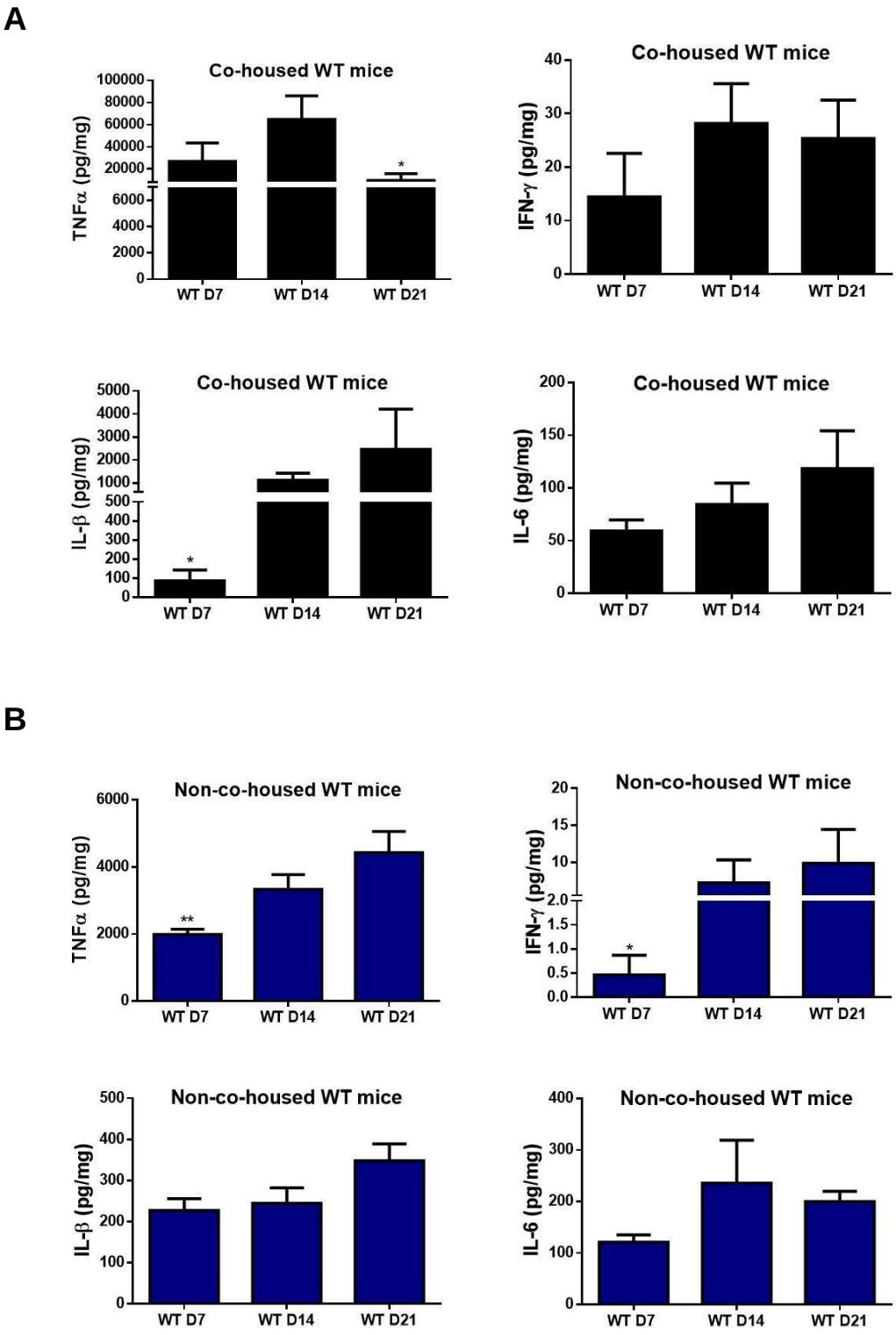

Figure 3. 15: Cytokine production in co-housed vs non-co-housed WT mice. Mice were infected with $2x10^5$ *P. murina* and cytokine production was measured over time.
A) Cytokine production in co-housed mice. B) Cytokine production measured in non-co-housed mice. The results are expressed as mean ± SEM (n = 5 mice per time point). Significant differences (* $p<0.05$, ** $p<0.01$) were determined using the unpaired two-tailed student's t- tests comparing both D7 and D21 against D14. Data shown represents one individual experiment. Figure 3.15A is also included in figure 3.8A

3.14. Co-housed DCAR mice

Cohabitation influenced fungal burden detected in DCAR-deficient mice, particularly, at day 7. When *P. murina* lung burden were quantified by qPCR, DCAR-deficient that were co-housed with WT mice for two weeks prior to infection presented with lower fungal burden at day 7 compared to WT mice (Figure 3.16A). However, when these mice were kept in separate cages before infection, this resulted in DCAR$^{-/-}$ mice presenting with a higher fungal load at day 7 compared to WT mice (Figure 3.16B). Owing to these variabilities, all our experimental mice were co-housed for two weeks before infection.

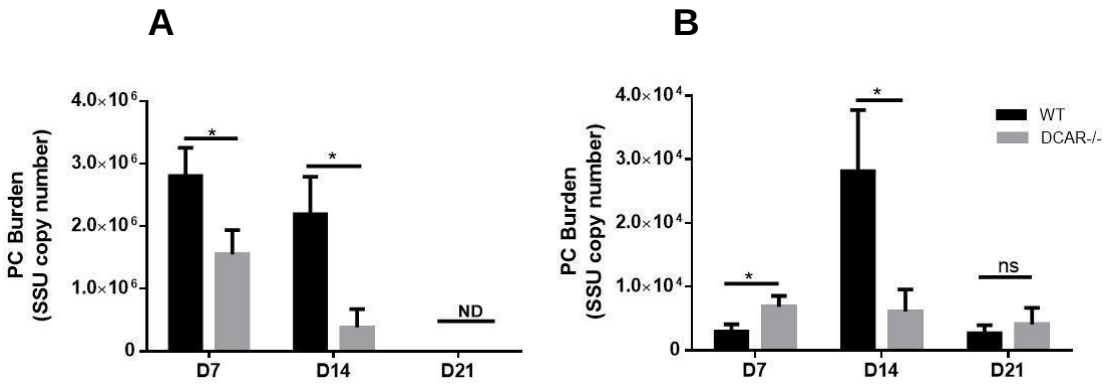

Figure 3. 16: *Pneumocystis murina* burden measured in co-housed and non-co-housed mice. *P. murina* burden was detected by qPCR at D7, D14, and D21. A) Fungal burden detected in DCAR and WT mice that were co-housed for 2 weeks prior to infection. B) Fungal burden detected in non-co-housed DCAR and WT mice. The results shown indicate the mean ± SEM of the values of five mice per time point in each group. Significant differences (* $p<0.05$) were determined using the unpaired one-tailed student's t-tests. Data shown represents one individual experiment. Figure 3.16A is also included in Figure 3.1A(ii).

Overall, the importance of experimental animal cohabitation has been clearly demostrated in this study. The differences observed in fungal burden were as a result of variations, particularly, in celluar recruitment. Whether these differences were as a consequence of microbiome exchange or other external factors, such as diet and water, remains to be determined. We do, however, show that co-housing is a critical component in animal research studies, which aims to standardise the base line of animals prior to infection.

Discussion

Chapter 4. Discussion, Future studies & Conclusion

4.1. DCAR in *Pneumocystis murina* infection

Pneumocystis pneumonia is a severe form of pneumonia of immunocompromised hosts caused by an opportunistic fungus *Pneumocystis jirovecii.* Host immune responses during infection are mediated by, but not limited to, C-type lectin receptors (CLRs). These receptors are expressed by several myeloid cells of the innate immune system which in turn triggers and primes the adaptive immune response. Increasing evidence suggests roles for CLRs such as Dectin-1 and Mincle during *Pneumocystis* infection(60, 69), we therefore used an established *P. murina* mouse model of infection to investigate the role of a newly described CLR, Dendritic Cell Immunoactivating Receptor (DCAR), during infection.

Firstly, we confirmed the deletion of the *Clec4b1* gene to ensure that the mice were globally deficient of DCAR. The behaviour and growth of the mice were not altered by the deletion of this gene. This was similarly shown by our collaborator; Sho Yamasaki (Japan) (71), where they described the role of DCAR in mycobacterial infection. In this study they found that DCAR is an important receptor for the mycobacteria ligand Phosphatidyl-inositol mannosides (PIMs). DCAR-deficient mice presented with high bacterial burden which was characterised by impaired cytokine secretion and minimal cellular recruitment (71).

Considering that DCAR is a CLR and that these receptors are important in *Pneumocystis* recognition, we investigated the role of DCAR by determining the disease progression in infected mice. Using qPCR to determine the fungal burden we show that DCAR$^{-/-}$ mice are more resistant to infection in comparison to WT mice. The low organism burden detected in DCAR$^{-/-}$ mice over the following timepoints: day7 and 14, served as clear indication of an advantageous effect of DCAR deletion in mice. This is in contrast with the role of this receptor during mycobacterial infection, as described above, where a deficiency in DCAR resulted in an increased bacterial load in mice (71). This could be due to the differences in the nature of infection between *Mycobacterium tuberculosis*, which is an intracellular pathogen, and *P. murina*

which is an extracellular organism. Interestingly, the role of DCAR is seemingly inversely related to that of Dectin-1 during *P. murina* infection. While Dectin-1 functions as an important *Pneumocystis* receptor that initiates host protective immunity (69), DCAR appears to predispose mice to infection. Comparably with the reports that Dectin-1 deficiency enables mice to clear mycobacterial infection more efficiently compared to WT mice (87), DCAR deficiency reduces fungal burden and potentially enhances protective immunity in mice.

Upon *P. murina* infection inflammatory cells are recruited to the site of infection to eliminate the pathogen. In this study we demonstrated the recruitment and localisation of cells using the H&E stain. Notably, the stain revealed extensively pronounced cellular infiltrates surrounding the peribronchiolar and perivascular regions of DCAR-deficient mice, particularly at day 21 post-infection. These observations were further supported by the observed decreasing trend of free alveolar space in these mice. These are characteristic of an asthmatic inflammation which have been previously reported during *Pneumocystis* infection (88). To further delineate the basis for the differences in fungal burden observed in DCAR-deficient and WT mice, we determined myeloid cell recruitment over the course of infection by flow cytometry. Alveolar macrophages are the undisputed key players during *Pneumocystis* infection as they recognize *Pneumocystis'* major surface antigen, gpA, through the mannose receptor (MR), thereby facilitating phagocytosis and instant killing of the organism (89). Furthermore, in immunocompromised patients there exists an inverse correlation in *Pneumocystis jirovecii* burden and the number of inflammatory cells present in the lungs (90). Indeed, alveolar macrophages were significantly increased 7 days post-infection in DCAR$^{-/-}$mice which corresponded to the reduced fungal load in these mice. Therefore, these results reflect a central role for alveolar macrophages during *P. murina* infection, which in our study was fostered by the deletion of DCAR.

Myeloid cells such as alveolar macrophages, in addition to their phagocytic function, further serve as antigen presenting cells possessing the ability to trigger an acquired immune response when a pathogenic organism is inhaled (3). Certainly, CD4^{+} T cells were the main cells of interest in our study as it is well-known that a deficiency in these cells predisposes the host to

Pneumocystis infection (63, 91). When analysing the profile of lymphocytes recruited into the lungs, we found that the DCAR-deficient mice presented with significantly high number of T cells at day 7 post-infection. The increased cellular recruitment trend was maintained at 14 days post-infection. Additionally, these T cells were in an activated state, suggesting that they could efficiently execute their effector function. These results hint to the importance of alveolar macrophages, which were significantly higher 7 days post-infection, as antigen presenters to T cells. These results further suggest a critical role of alveolar macrophages as triggers of adaptive immunity. Accordingly, we could postulate that the reduced fungal burden observed in DCAR$^{-/-}$ mice was due to the efficient crosstalk between the innate and adaptive immune system through alveolar macrophage-T cell interaction, which could be accredited to or was enhanced by the deletion of DCAR.

DCAR deficiency in mice infected with mycobacteria impairs the production of proinflammatory cytokines, including IFN-γ and IL-12 (71). The importance of these cytokines during *Pneumocystis* infection is well documented. While IFN-γ is not directly linked to *Pneumocystis* control, it is an important regulator of exacerbated inflammatory responses mounted against *Pneumocystis* thus preventing lung pathology (92). Conversely, IL-12 drives cellular recruitment and significantly enhances *P. murina* clearance in immunocompromised mice (93). In our study the overall trend of the proinflammatory cytokines was increased, however, these differences were of no statistical significance. Of important to note was the increased trend of TNFα in DCAR$^{-/-}$ mice at day 7, which coincided with the observed increased number of AMs and neutrophils in these mice. Although TNFα does not exclusively orchestrate the recruitment of AMs and neutrophils to the site of infection, this cytokine has however been shown to play a crucial role in this process, and can thus further enhance antifungal immunity by these cells (94).

Another cytokine of importance during *P. murina* infection is IL-1β, which has been shown to promote proliferation of Th17 cells in WT immunocompetent mice, which are important in antifungal immunity (95). Consistent with these reports, IL-1β production levels showed mildly increased trend in DCAR-deficient mice at both day 7 and day 14 post-infection and was later reduced.

Moreover, IL-1β production is collaboratively induced by neutrophils and alveolar macrophages during respiratory viral infection (96), and alveolar macrophages were significantly increased in DCAR$^{-/-}$ mice, while neutrophils also showed a mild increased trend 7 days post-infection in our study. Therefore, taken together our data shows that DCAR deficiency during *P. murina* infection promotes alveolar macrophage response and neutrophil recruitment which in turn drive proinflammatory responses through the induction of cytokines that drive Th1 and Th17 proliferation, which could provide an explanation for the accelerated *P. murina* clearance.

Inflammatory responses remain important in *Pneumocystis* clearance, however, when not regulated they can cause severe lung tissue injury. This phenomenon was clearly shown in IL-10-deficient mice infected with *Pneumocystis*. Upon infection these mice efficiently cleared *Pneumocystis*, however, IL-10 deletion perpetuated inflammation consequently causing lung pathology (97). In our study IL-10 production was significantly impaired in DCAR$^{-/-}$ mice at day 7, and this trend was maintained throughout the course of infection. Coinciding with these diminished levels of IL-10 in DCAR-deficient mice was the exaggerated infiltration of cells observed at a later timepoint when mice had cleared the infection. The pronounced inflammation was further substantiated by a trend of decreased free alveolar spaces observed in DCAR$^{-/-}$ at day 21. Taken together, these results thus infer that in the absence of DCAR, mice experience increased inflammatory responses that enhance pathogen clearance. However, if these lead to a negative outcome for lung function remains to be determined. Contrarily, it is possible that what we observe in DCAR$^{-/-}$ mice is the required immune response that efficiently clears *Pneumocystis*. Suggesting that there is a defect in pathogen recognition in WT mice, therefore the immune response is not as efficient as expected. This is further exacerbated in immunocompromised mice.

Secretion of airway mucus is a defense mechanism employed to entrap foreign invading particles and pathogens. During bacterial pneumonia mucus secretion is said to prevent disease progression and fosters pathogen clearance (98). The latter is true during primary *Pneumocystis* infection, where mucin hypersecretion reportedly plays a defensive role (99). In contrast,

progressive mucus hypersecretion has been shown to have a detrimental effect resulting in lung diseases such as asthma and chronic obstructive pulmonary disease (100). In our study DCAR-deficient mice showed pronounced mucus production which was maintained until the last experimental time point (day 21). Considering that the fungal burden was reduced in DCAR-deficient mice compared to WT throughout the experimental period, we could speculate that mucus production in these mice played a protective role. However, the seemingly decreased percentage of free alveolar spaces observed in these mice may serve as an indication of the importance of this receptor as an immune modulator. Therefore, these data suggest that DCAR deletion drives mucus production, in turn accelerating *P. murina* clearance in mice, however, DCAR deficiency may ultimately be the source of impaired lung function.

4.2. DCAR in the early host immune response

Considering that DCAR is an innate receptor, next we looked at the early cell recruitment and cytokine production. At 48hrs post-infection we observed no differences in the number of alveolar macrophages, dendritic cells, neutrophils and inflammatory monocytes in the BAL from both PBS treated and *P. murina* infected WT and DCAR$^{-/-}$ mice. Furthermore, the overall trend of cytokine production showed no significant differences in DCAR$^{-/-}$ mice, with the exception of IL-6 which was significantly increased in PBS treated WT mice. An interesting observation was that of increased IL-1β in PBS treated control DCAR$^{-/-}$ mice at 48 hrs. This could suggest that DCAR deletion in mice induces IL-1β production, in turn granting our transgenic mice an advantage over WT mice in *P. murina* clearance. However, these experiments were only done once and would need to be confirmed. Our observations signify the influence of DCAR deletion in early recruitment of principal cells, and further imply a potential role for IL-1β as an accessory in the first line of defense during *P. murina* infection.

4.3. The effect of cohousing on the immune response during *P. murina* infection

The assessment of the role that cohabitation has on immune phenotypes and disease outcome is an important growing trend in the field of animal research. Recent studies have shown that cohabitation can influence phenotypic variabilities that may be due to not only genetic modification of mice but also external environmental factors such as microbiome (85, 101). Overall, the cytokine profiles in our study were similar between mice that were cohoused and those that were not. However, there were discrepancies in cellular recruitment as our results demonstrated that both the innate and adaptive immune cellular profiles were different in cohoused mice compared to those that were not. These differences in the immune responses further translated into variabilities in fungal burden in mice that were cohoused and those that were not. Our findings concur with those reported by Gauguet *et.al* (2015) whereby susceptibility of mice to *Staphylococcus aureus* was abrogated by 14 days of cohousing (101). Therefore, although these experiments were only done once, they guided our decision to cohouse all experimental animals.

4.4. Future studies

Our data has provided valuable insight into the role of DCAR in *Pneumocystis* infection. However, to fully understand these processes additional questions remain. Of interest would be to fully characterise the role of IL-1β in naïve DCAR-deficient mice. It has been previously reported that IL-1β promotes IL-17 production by Th17 cells which are important antifungal T cells (95). Therefore, we would repeat the 48 hours experiment to confirm the higher levels of IL-1β in PBS only treated DCAR-deficient mice. Additionally, we could analyse the IL-1β levels in naïve lung tissue. Here it would be valuable to determine the IL-17 production in *P. murina* infected mice.

We could also further analyse the increased cellular response detected in DCAR-deficient mice, later in infection and how this corresponds to the Th2 responses mentioned. Firstly, we would quantify mucus production as a

means of verifying whether the cumulative mucus secretion observed in DCAR-deficient mice caused any impaired lung functionality. As mucus production is associated with a Th2 response, secondly, we could expand our data to include these responses. This could include measuring serum antibody production including IgG and IgE. Furthermore, we would look at Th2 cytokine production by ELISA and qPCR, specifically IL-13 which is associated with mucus production. Furthermore, we could measure IL-5 production and the associated eosinophil recruitment. Therefore, we would include Sirius red staining on our histology sections for eosinophils and also determine if there is eosinophilia in our FACS analysis ($CD11c^{-}$ $Siglecf^{+}$ cell population). Considering that prolonged inflammatory responses can eventually lead to decreased lung functionality, we would also determine whether the decreased free alveolar spaces observed in $DCAR^{-/-}$ mice at day 21 results in altered lung capacity using a flexiVent (SCIREQ, Canada, currently available at UCT) which measures different parameters in the lung including resistance and compliance.

We could also explore alveolar macrophage depletion to determine whether an early increase in these cells observed in DCAR-deficient mice is the primary source of protective immunity in these mice. Alveolar macrophage depletion would be through intranasal administration of Clodronate and we would determine *P. murina* burden by qPCR at an early timepoint.

Future work will also consider immune suppression of mice through $CD4^{+}$ T cell depletion as a means of establishing whether this receptor is required during disease manifestation in immunocompromised hosts. This would be based on the observations that the critical role of CLRs such as Dectin-1 and Mincle is more apparent during chronic *P. murina* infection. For example, the absence of Dectin-1 renders the mice more sensitive to infection which is indicated by high fungal burden in these mice at both day 7 and 14. However, these mice clear infection by day 20. In contrast, Dectin-1-deficient mice that lack T cells suffer from chronic infection as indicated by the detection of fungi four months post-infection (69). Parallel to this, are reports on Mincle-deficient mice, that have enhanced *P. murina* burden following $CD4^{+}$ T cell depletion (60).

4.5. Conclusion

We have shown for the first time that DCAR-deficient mice are more resistant to *P. murina* infection. The absence of DCAR led to a significantly low fungal burden, which was associated with a significantly higher immune cell infiltration into the site of infection. This in turn translated into increased T cell recruitment and activation. Furthermore, the cytokine production pattern was higher in DCAR-deficient mice, with a notable increase in IL-1β early post-infection. However, despite these enhanced immune responses in DCAR-deficient mice, infection was eventually controlled in both DCAR-deficient and WT mice by day 21. Additionally, DCAR-deficient mice exhibited elevated mucus production throughout the course of infection, suggesting that DCAR-deficiency likely promotes Th2 responses. Overall, DCAR is a potential driver of susceptibility of mice to *P. murina* infection. However, while the lack of this receptor drives protective immunity in mice during *P. murina* infection, characterised by increased alveolar macrophage, DCs, neutrophils, eosinophils, inflammatory monocytes and T cell recruitment, it may also be important in inflammatory response regulation. The mechanism by which the deletion of this receptor affords these mice ability to efficiently clear *P. murina* remains to be determined.

Appendices

Appendix A: Solutions

Lavage buffer

- 100µl EDTA
- 50ml 1x PBS

ELISA

1X Phosphate Buffer Saline (PBS)

- 100 PBS Tablets (Thermo Scientific™ Oxoid™)
- 10L dH2O

Coating buffer

- 1X PBS (pH 8.5)
- Capture antibody (1:250)

Wash buffer

- 0.05% Tween 20 (50 ml)
- 1x PBS (10 L)
- pH to 7.4

Blocking buffer

- 2% bovine serum albumin (BSA)
- 0.2g NaN_3
- Make up to 1000ml with 1x PBS and store at 4°C

Diluent buffer

- 1% BSA
- 0.2g NaN_3
- 1x PBS
- pH to 7.4

HRP Substrate Buffer

- Mix 50% of each TMB Substrate reagent set (BD Fisher Scientific)
- Substrate reagent A contains hydrogen peroxide
- Substrate reagent B containing 3,3′, 5,5′ tetramethylbenzidine (TMB) in an organic solvent

Flow cytometry

Digestion buffer

- 120 ml DMEM
- 0.0226 g Collagenase Type II, powder (Thermo Fisher Scientific)
- 31.2 µl DNase I

FACS buffer

- 1X PBS
- 0.5-1% BSA
- 0.1% NaN3

Red cell lysis buffer

- 5 mM EDTA
- 150 mM NaCl
- 10 % glycerol
- 25 mM Tris-Cl pH 7.5
- 0.1 % SDS
- 1 % Triton –X 100
- 0.5 % Non idet P-40
- 0.5 % Deoxycholate
- 5 mM PMSF

Fixation buffer

- 4g NaOH
- 100ml 1x PBS

- 20g paraformaldehyde
- Adjust to 7.2 and make up to 1000ml with
- Filter to sterilize

PCR Master mix

- 10 µl 2X SsoAdvanced Universal Probes supermix
- 0.5 µl 40X primer mix
- 4.5 µl RNAse free H_2O

Genotyping

1.6 % agarose gels

- 8g agarose
- 25ml 10x TBE buffer (0.5x)
- Make up to 500ml with dH_2O
- Dissolve in a microwave

10 x Stock Tris borate ethylene di-amino tetra acetic acid (TBE)

- 108g Tris (base)
- 55g Boric acid and
- 40ml 0.5M EDTA
- 1000ml of water sterilized through a 0.45µm filter (Millipore Corporation, Bedford, USA) and stored at room temperature.
- 1x TBE = 1:9 (10x TBE: dH_2O)

Histology

10% formalin

- 100ml formaldehyde (40% w/v formaldehyde solution)
- 900ml PBS (pH 7.4)
- Store in a dark bottle

Supplementary figure

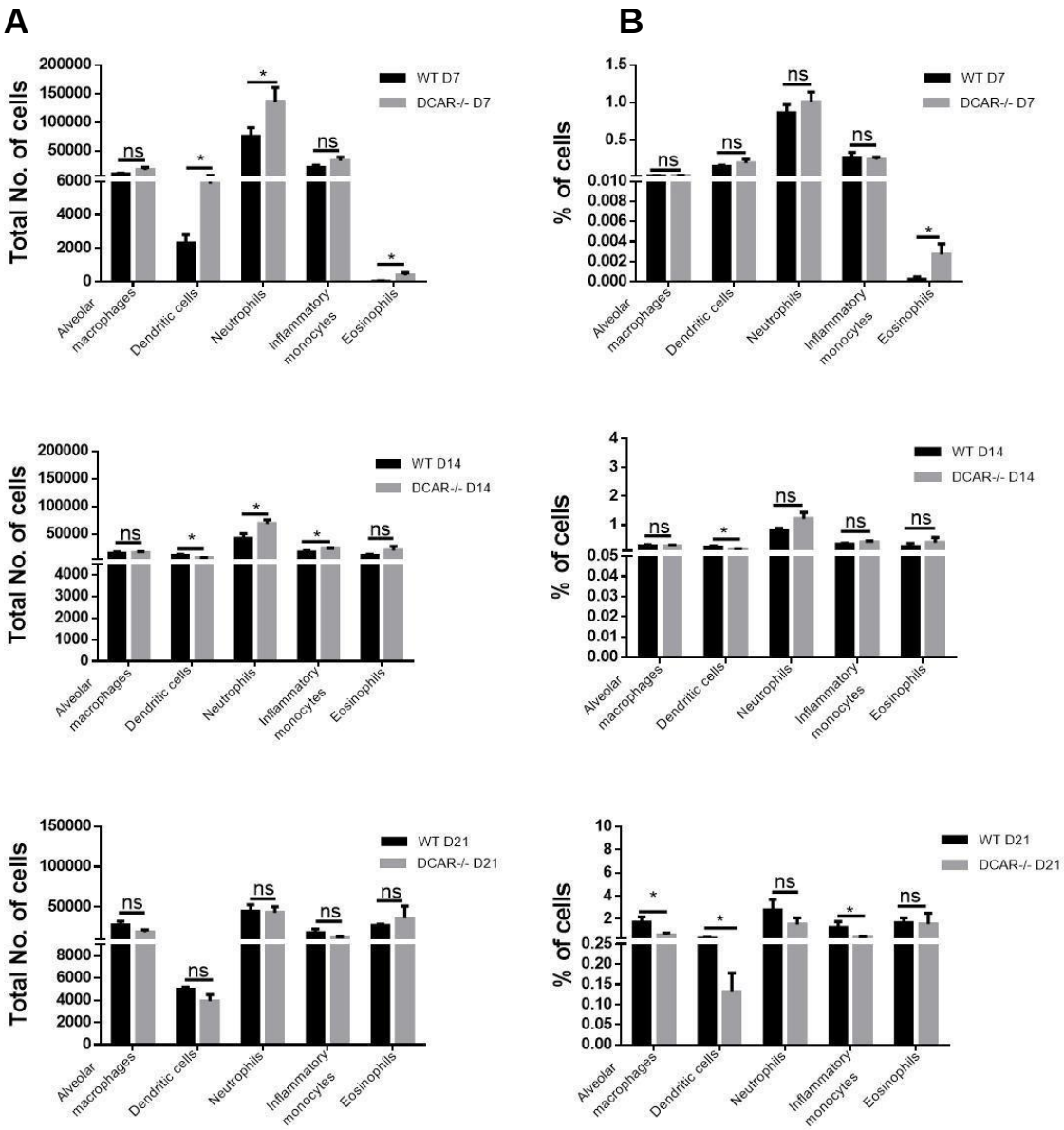

Figure 1: Cellular responses post P. murina infection was measured by flow cytometry. WT and DCAR-/- mice were infected with 2x105 of P. murina and sacrificed at the indicated timepoints. The graphs show a comparison between absolute numbers and percentages. A&B) Cellular responses in the lungs of both WT and DCAR-/- were measured overtime. The results are expressed as mean ± SEM (n = 5 mice/strain per time point). Significant differences (* $p<0.05$) were determined using the unpaired one-tailed student's t- tests. Data shown are of an individual experiment that repeats data shown in Figure 3.6.

References

1. Linke MJ, Ashbaugh A, Collins MS, Lynch K, Cushion MT. Characterization of a distinct host response profile to Pneumocystis murina asci during clearance of pneumocystis pneumonia. Infect Immun. 2013;81(3):984-95.

2. Stringer JR, Beard CB, Miller RF, Wakefield AE. A New Name for Pneumocystis from Humans and New Perspectives on the Host-Pathogen Relationship. Emerging Infectious Diseases. 2002;8(9):891-6.

3. Kelly MN, Shellito JE. Current understanding of Pneumocystis immunology. Future microbiology. 2010;5(1):43-65.

4. Aliouat-Denis C-M, Chabé M, Demanche C, Aliouat EM, Viscogliosi E, Guillot J, et al. Pneumocystis species, co-evolution and pathogenic power. Infection, Genetics and Evolution. 2008;8(5):708-26.

5. Kaur R, Wadhwa A, Bhalla P, Dhakad MS. Pneumocystis pneumonia in HIV patients: a diagnostic challenge till date. Med Mycol. 2015;53(6):587-92.

6. Ma L, Cissé OH, Kovacs JA. A Molecular Window into the Biology and Epidemiology of Pneumocystis spp. Clinical Microbiology Reviews. 2018;31(3).

7. Helweg-Larsen J. Pneumocystis jiroveci Applied molecular microbiology, epidemiology and diagnosis. D A N I SH MED ICAL BUL L E T IN. 2004;51(3):251-73.

8. Kutty G, Davis AS, Ferreyra GA, Qiu J, Huang DW, Sassi M, et al. β-Glucans Are Masked but Contribute to Pulmonary Inflammation During Pneumocystis Pneumonia. J Infect Dis. 2016;214(5):782-91.

9. Evans HM, Bryant GL, Garvy BA. The Life Cycle Stages of Pneumocystis murina Have Opposing Effects on the Immune Response to This Opportunistic Fungal Pathogen. Infection and immunity. 2016;84(11):3195-205.

10. Martinez A, Halliez MCM, Moukhtar Aliouat E, Chabé M, Standaert-Vitse A, Fréalle E, et al. Growth and Airborne Transmission of Cell-Sorted Life Cycle Stages of Pneumocystis carinii. PLoS ONE. 2013;8(11): e79958.

11. Beck JM, Cushion MT. Pneumocystis workshop: 10th anniversary summary. Am Soc Microbiol; 2009.

12. Global Action Fund For Fungal Infections. Fungal Disease Frequency n.d. [Available from: http://www.gaffi.org/why/fungal-disease-frequency.

13. Beck JM, Warnock ML, Kaltreider HB, Shellito JE. Host Defenses Against Pneumocystis carinii in Mice Selectively Depleted of CD4+ Lymphocytes. Chest. 1993;103(2, Supplement):116S-8S.

14. Kharsany ABM, Karim QA. HIV Infection and AIDS in Sub-Saharan Africa: Current Status, Challenges and Opportunities. The open AIDS journal. 2016; 10:34-48.

15. Roux A, Canet E, Valade S, Gangneux-Robert F, Hamane S, Lafabrie A, et al. Pneumocystis jirovecii pneumonia in patients with or without AIDS, France. Emerging infectious diseases. 2014;20(9):1490-7.

16. Wickramasekaran RN, Jewell MP, Sorvillo F, Kuo T. The changing trends and profile of pneumocystosis mortality in the United States, 1999-2014. Mycoses. 2017;60(9):607-15.

17. Maini R, Henderson KL, Sheridan EA, Lamagni T, Nichols G, Delpech V, et al. Increasing Pneumocystis pneumonia, England, UK, 2000-2010. Emerging infectious diseases. 2013;19(3):386-92.

18. Rubaihayo J, Tumwesigye NM, Konde-Lule J. Trends in prevalence of selected opportunistic infections associated with HIV/AIDS in Uganda. BMC Infectious Diseases. 2015;15(1):187.

19. Kottom TJ, Hebrink DM, Jenson PE, Nandakumar V, Wüthrich M, Wang H, et al. The Interaction of Pneumocystis with the C-Type Lectin Receptor Mincle Exerts a Significant Role in Host Defense against Infection. The Journal of Immunology. 2017;198(9):3515.

20. Gajdusek DC. Pneumocystis Carinii—Etiologic Agent Of Interstitial Plasma Cell Pneumonia Of Premature And Young Infants. Pediatrics. 1957;19(4):543.

21. Vanek J. [Atypical (interstitial) pneumonia in children caused by Pneumocystis carinii]. Casopis lekaru ceskych. 1951;90(38):1121-4.

22. Alison M, Jens DL, Henry M, Peter DW, Debra LH, Toni F, et al. Current Epidemiology of Pneumocystis Pneumonia. Emerging Infectious Disease journal. 2004;10(10):1713.

23. Sepkowitz KA, Brown AE, Telzak EE, Gottlieb S, Armstrong D. Pneumocystis carinii pneumonia among patients without aids at a cancer hospital. JAMA. 1992;267(6):832-7.

24. Martin SI, Fishman JA. Pneumocystis pneumonia in solid organ transplant recipients. American journal of transplantation: official journal of the American Society of Transplantation and the American Society of Transplant Surgeons. 2009;9 Suppl 4: S227-33.

25. Huang L, Cattamanchi A, Davis JL, Boon Sd, Kovacs J, Meshnick S, et al. HIV-Associated Pneumocystis Pneumonia. Proceedings of the American Thoracic Society. 2011;8(3):294-300.

26. Barbosa AN, Souza LR. Occurrence of pneumocystis pneumonia in hiv-infected patients and the interference of the highly active antiretroviral therapy. Journal of Venomous Animals and Toxins including Tropical Diseases. 2008; 14:152-60.

27. Lu Y, Ling G, Qiang C, Ming Q, Wu C, Wang K, et al. PCR Diagnosis of Pneumocystis Pneumonia: A Bivariate Meta-Analysis. Journal of Clinical Microbiology. 2011;49(12):4361-

3.

28. Alison Morris KW, 2 Kamyar Afshar,2 and Laurence Huang3. Epidemiology and Clinical Significance of Pneumocystis Colonization. The Journal of Infectious Diseases. 2008(197):10-7.

29. Kanne JP, Yandow DR, Meyer CA. Pneumocystis jiroveci Pneumonia: High-Resolution CT Findings in Patients With and Without HIV Infection. American Journal of Roentgenology. 2012;198(6): W555-W61.

30. Huang L, Cattamanchi A, Davis JL, Boon Sd, Kovacs J, Meshnick S, et al. HIV-Associated Pneumocystis Pneumonia. Proceedings of the American Thoracic Society. 2011;8(3):294-300.

31. Florence Robert-Gangneux, Sorya Belaz, Matthieu Revest,Pierre Tattevin, Stéphane Jouneau, Olivier Decaux,Sylviane Chevrier bYLT, Jean-Pierre Gangneux. Diagnosis of Pneumocystis jirovecii Pneumonia in Immunocompromised Patients by Real-Time PCR: a 4-Year Prospective Study. Journal of Clinical Microbiology. 2014;52(9):3370–6.

32. Fillaux J, Malvy S, Alvarez M, Fabre R, Cassaing S, Marchou B, et al. Accuracy of a routine real-time PCR assay for the diagnosis of Pneumocystis jirovecii pneumonia. Journal of Microbiological Methods. 2008;75(2):258-61.

33. Botterel F, Cabaret O, Foulet F, Cordonnier C, Costa J-M, Bretagne S. Clinical Significance of Quantifying Pneumocystis jirovecii DNA by Using Real-Time PCR in Bronchoalveolar Lavage Fluid from Immunocompromised Patients. Journal of Clinical Microbiology. 2012;50(2):227-31.

34. Onishi A, Sugiyama D, Kogata Y, Saegusa J, Sugimoto T, Kawano S, et al. Diagnostic accuracy of serum 1,3-β-D-glucan for pneumocystis jiroveci pneumonia, invasive candidiasis, and invasive aspergillosis: systematic review and meta-analysis. Journal of clinical microbiology. 2012;50(1):7-15.

35. Thomas CF, Jr., Limper AH. Current insights into the biology and pathogenesis of Pneumocystis pneumonia. Nature reviews Microbiology. 2007;5(4):298-308.

36. Adolescents PoOIiH-IAa. Guidelines for the prevention and treatment of opportunistic infections in HIVinfected adults and adolescents: recommendations from the Centers for Disease Control and Prevention, the National Institutes of Health, and the HIV Medicine Association of the Infectious Diseases Society of America Available at

http://aidsinfo.nih.gov/contentfiles/lvguidelines/adult_oi.pdf.2017

37. De Stefano JA, Myers JD, Du Pont D, Foy JM, Theus SA, Walzer PD. Cell wall antigens of Pneumocystis carinii trophozoites and cysts: purification and carbohydrate analysis of these glycoproteins. The Journal of eukaryotic microbiology. 1998;45(3):334-43.

38. Robert F. Miller JLN, Elizabeth L. Corbetf, J. Mark Felton and, Cock KMD. Pneumocystis carinii infection: current treatment and prevention. Journal of Antimicrobial Chemotherapy. 1996; 37:33-53.

39. Delves PJ, Roitt IM. The Immune System. New England Journal of Medicine. 2000;343(1):37-49.

40. Gonzalez S, González-Rodríguez AP, Suárez-Álvarez B, López-Soto A, Huergo-Zapico L, Lopez-Larrea C. Conceptual aspects of self and nonself discrimination. Self/nonself. 2011;2(1):19-25.

41. Warrington R, Watson W, Kim HL, Antonetti FR. An introduction to immunology and immunopathology. Allergy, Asthma, and Clinical Immunology: Official Journal of the Canadian Society of Allergy and Clinical Immunology. 2011;7(Suppl 1): S1-S.

42. Medzhitov R, Janeway CA. Innate immunity: impact on the adaptive immune response. Current Opinion in Immunology. 1997;9(1):4-9.

43. Jr. RMaCAJ. Decoding the Patterns of Self and Nonself by the Innate Immune System. Reflections on Self: Immunity and Beyond. 2002; 296:298-300.

44. Gonzalez S, González-Rodríguez AP, Suárez-Álvarez B, López-Soto A, Huergo-Zapico L, Lopez-Larrea C. Conceptual aspects of self and nonself discrimination. Self Nonself. 2011;2(1):19-25.

45. Akira S, Uematsu S, Takeuchi O. Pathogen Recognition and Innate Immunity. Cell. 2006;124(4):783-801.

46. Fukui M, Imamura R, Umemura M, Kawabe T, Suda T. Pathogen-Associated Molecular Patterns Sensitize Macrophages to Fas Ligand-Induced Apoptosis and IL-1β Release. The Journal of Immunology. 2003;171(4):1868.

47. Bello-Irizarry SN, Wang J, Olsen K, Gigliotti F, Wright TW. The alveolar epithelial cell chemokine response to pneumocystis requires adaptor molecule MyD88 and interleukin-1 receptor but not toll-like receptor 2 or 4. Infection and immunity. 2012;80(11):3912-20.

48. Takeuchi O, Akira S. Pattern Recognition Receptors and Inflammation. Cell. 2010;140(6):805-20.

49. Hoving JC, Wilson GJ, Brown GD. Signalling C-Type lectin receptors, microbial recognition and immunity. Cellular Microbiology. 2014;16(2):185-94.

50. Geijtenbeek TBH, Gringhuis SI. Signalling through C-type lectin receptors: shaping immune responses. Nature Reviews Immunology. 2009; 9:465.

51. Dambuza IM, Brown GD. C-type lectins in immunity: recent developments. Current Opinion in Immunology. 2015; 32:21-7.

52. Gazi U, Rosas M, Singh S, Heinsbroek S, Haq I, Johnson S, et al. Fungal recognition enhances mannose receptor shedding through dectin-1 engagement. Journal of Biological Chemistry. 2011;286(10):7822-9.

53. McGreal EP, Rosas M, Brown GD, Zamze S, Wong SYC, Gordon S, et al. The carbohydrate-recognition domain of Dectin-2 is a C-type lectin with specificity for high mannose. Glycobiology. 2006;16(5):422-30.

54. Heyl KA, Klassert TE, Heinrich A, Müller MM, Klaile E, Dienemann H, et al. Dectin-1 Is Expressed in Human Lung and Mediates the Proinflammatory Immune Response to Nontypeable Haemophilus influenzae. mBio. 2014;5(5): e01492-14.

55. Hardison SE, Brown GD. C-type Lectin Receptors Orchestrate Anti-Fungal Immunity. Nature immunology. 2012;13(9):817-22.

56. Harris JR, Marston BJ, Sangrujee N, DuPlessis D, Park B. Cost-Effectiveness Analysis of Diagnostic Options for Pneumocystis Pneumonia (PCP). PLoS ONE. 2011;6(8): e23158.

57. Drummond RA, Saijo S, Iwakura Y, Brown GD. The role of Syk/CARD9 coupled C-type lectins in antifungal immunity. European Journal of Immunology. 2011;41(2):276-81.

58. Plato A, Hardison SE, Brown GD. Pattern recognition receptors in antifungal immunity. Seminars in Immunopathology. 2015;37(2):97-106.

59. Kerscher B, Wilson GJ, Reid DM, Mori D, Taylor JA, Besra GS, et al. Mycobacterial receptor, Clec4d (CLECSF8, MCL), is coregulated with Mincle and upregulated on mouse myeloid cells following microbial challenge. Eur J Immunol. 2016;46(2):381-9.

60. Kottom TJ, Hebrink DM, Jenson PE, Nandakumar V, Wüthrich M, Wang H, et al. The interaction of pneumocystis with the C-type lectin receptor Mincle exerts a significant role in host defense against infection. The Journal of Immunology. 2017;198(9):3515-25.

61. Kottom TJ, Hebrink DM, Jenson PE, Marsolek PL, Wüthrich M, Wang H, et al. Dectin-2 Is a C-Type Lectin Receptor that Recognizes Pneumocystis and Participates in Innate Immune Responses. American Journal of Respiratory Cell and Molecular Biology. 2018;58(2):232-40.

62. Paola Castiglioni MG, Xochitl Cortez-Gonzalez and Maurizio Zanetti. CD8 T cell priming by B lymphocytes is CD4 help dependent. European journal of immunology. 2005;35(5):1360–70.

63. Swain SD, Meissner NN, Harmsen AG. CD8 T cells modulate CD4 T-cell and eosinophil-mediated pulmonary pathology in pneumocystis pneumonia in B-cell-deficient mice. The American journal of pathology. 2006;168(2):466-75.

64. Zhu J, Paul WE. CD4 T cells: fates, functions, and faults. Blood. 2008;112(5):1557-69

65. Wan YY, Flavell RA. How diverse--CD4 effector T cells and their functions. Journal of molecular cell biology. 2009;1(1):20-36.

66. van de Veerdonk FL, Netea MG. T-cell Subsets and Antifungal Host Defenses. Current fungal infection reports. 2010;4(4):238-43.

67. Curtis MM, Way SS. Interleukin-17 in host defence against bacterial, mycobacterial and fungal pathogens. Immunology. 2009;126(2):177-85.

68. Ripamonti C, Bishop LR, Kovacs JA. Pulmonary Interleukin-17-Positive Lymphocytes Increase during Pneumocystis murina Infection but Are Not Required for Clearance of Pneumocystis. Infection and immunity. 2017;85(7): e00434-16.

69. Saijo S, Fujikado N, Furuta T, Chung S-h, Kotaki H, Seki K, et al. Dectin-1 is required for host defense against Pneumocystis carinii but not against Candida albicans. Nature Immunology. 2006; 8:39.

70. Hoving JC. Pneumocystis and interactions with host immune receptors. PLoS pathogens. 2018;14(2): e1006807-e.

71. Toyonaga K, Torigoe S, Motomura Y, Kamichi T, Hayashi JM, Morita YS, et al. C-Type Lectin Receptor DCAR Recognizes Mycobacterial Phosphatidyl-Inositol Mannosides to Promote a Th1 Response during Infection. Immunity. 2016;45(6):1245-57.

72. Kanazawa N, Tashiro K, Miyachi Y. Signaling and immune regulatory role of the dendritic cell immunoreceptor (DCIR) family lectins: DCIR, DCAR, dectin-2 and BDCA-2. Immunobiology. 2004;209(1):179-90.

73. Kanazawa N. Dendritic cell immunoreceptors: C-type lectin receptors for pattern-recognition and signaling on antigen-presenting cells. Journal of Dermatological Science. 2007;45(2):77-86.

74. Osorio F, Reis e Sousa C. Myeloid C-type Lectin Receptors in Pathogen Recognition and Host Defense. Immunity. 2011;34(5):651-64.

75. Tashiro K, Inaba K, Miyachi Y. Dendritic cell immunoactivating receptor, a novel C-type lectin immunoreceptor, acts as an activating receptor through association with Fc receptor γ chain. Journal of Biological Chemistry. 2003;278(35):32645-52.

76. Kaden SA, Kurig S, Vasters K, Hofmann K, Zaenker KS, Schmitz J, et al. Enhanced Dendritic Cell-Induced Immune Responses Mediated by the Novel C-Type Lectin Receptor mDCAR1. The Journal of Immunology. 2009;183(8):5069.

77. Kanazawa N, Okazaki T, Nishimura H, Tashiro Kei, Inaba K, Miyachi Y. DCIR Acts as an Inhibitory Receptor Depending on its Immunoreceptor Tyrosine-Based Inhibitory Motif11A preliminary report of these results was presented by the first author at the 61st annual meeting of SID in Chicago in the session “General Immunology”. Journal of Investigative Dermatology. 2002;118(2):261-6.

78. Feinberg H, Jégozuo SA, Rex MJ, Drickamer K, Weis WI, Taylor ME. Mechanism of pathogen recognition by human dectin-2. Journal of Biological Chemistry. 2017: jbc. M117. 799080.

79. Del Fresno C, Iborra S, Saz-Leal P, Martínez-López M, Sancho D. Flexible Signaling of Myeloid C-Type Lectin Receptors in Immunity and Inflammation. Frontiers in immunology. 2018; 9:804-.

80. Marakalala MJ, Ndlovu H. Signaling C-type lectin receptors in antimycobacterial immunity. PLOS Pathogens. 2017;13(6): e1006333.

81. Sakuma T, Ochiai H, Kaneko T, Mashimo T, Tokumasu D, Sakane Y, et al. Repeating pattern of non-RVD variations in DNA-binding modules enhances TALEN activity. Scientific reports. 2013; 3:3379.

82. Nakagawa Y, Sakuma T, NakagaTa N, YamaSaki S, Takeda N, Ohmuraya M, et al. Application of oocyte cryopreservation technology in TALEN-mediated mouse genome editing. Experimental animals. 2014;63(3):349-55.

83. Shellito J, Suzara V, Blumenfeld W, Beck J, Steger H, Ermak T. A new model of Pneumocystis carinii infection in mice selectively depleted of helper T lymphocytes. J Clin Invest. 1990;85(5):1686-93.

84. Rudmann DG, Preston AM, Moore MW, Beck JM. Susceptibility to Pneumocystis carinii in Mice Is Dependent on Simultaneous Deletion of IFN-γ and Type 1 and 2 TNF Receptor Genes. The Journal of Immunology. 1998;161(1):360-6.

85. Franklin CL, Ericsson AC. Microbiota and reproducibility of rodent models. Lab Anim (NY). 2017;46(4):114-22.

86. Caruso R, Ono M, Bunker ME, Núñez G, Inohara N. Dynamic and Asymmetric Changes of the Microbial Communities after Cohousing in Laboratory Mice. Cell Reports. 2019;27(11):3401-12. e3.

87. Marakalala MJ, Guler R, Matika L, Murray G, Jacobs M, Brombacher F, et al. The Syk/CARD9-coupled receptor Dectin-1 is not required for host resistance to Mycobacterium tuberculosis in mice. Microbes and Infection. 2011;13(2):198-201.

88. Meissner NN, Swain S, Tighe M, Harmsen A, Harmsen A. Role of Type I IFNs in Pulmonary Complications of Pneumocystis murina Infection. The Journal of Immunology. 2005;174(9):5462.

89. Ezekowitz RAB, Williams DJ, Koziel H, Armstrong MYK, Warner A, Richards FF, et al. Uptake of Pneumocystis carinii mediated by the macrophage mannose receptor. Nature. 1991;351(6322):155-8.

90. Iriart X, Witkowski B, Courtais C, Abbes S, Tkaczuk J, Courtade M, et al. Cellular and cytokine changes in the alveolar environment among immunocompromised patients during Pneumocystis jirovecii infection. Medical Mycology. 2010;48(8):1075-87.

91. Shellito J, Suzara VV, Blumenfeld W, Beck JM, Steger HJ, Ermak TH. A new model of Pneumocystis carinii infection in mice selectively depleted of helper T lymphocytes. Journal of Clinical Investigation. 1990;85(5):1686-93.

92. Hu T, Takamoto M, Hida S, Tagawa Y-i, Sugane K. IFN-γ deficiency worsen Pneumocystis pneumonia with Th17 development in nude mice. Immunology Letters. 2009;127(1):55-9.

93. Ruan S, McKinley L, Zheng M, Rudner X, D'Souza A, Kolls JK, et al. Interleukin-12 and host defense against murine Pneumocystis pneumonia. Infection and immunity. 2008;76(5):2130-7.

94. Filler SG, Yeaman MR, Sheppard DC. Tumor Necrosis Factor Inhibition and Invasive Fungal Infections. Clinical Infectious Diseases. 2005;41(Supplement_3): S208-S12.

95. Perez-Nazario N, Rangel-Moreno J, O'Reilly MA, Pasparakis M, Gigliotti F, Wright TW. Selective ablation of lung epithelial IKK2 impairs pulmonary Th17 responses and delays the clearance of Pneumocystis. J Immunol. 2013;191(9):4720-30.

96. Peiró T, Patel DF, Akthar S, Gregory LG, Pyle CJ, Harker JA, et al. Neutrophils drive alveolar macrophage IL-1β release during respiratory viral infection. Thorax. 2018;73(6):546-56.

97. Qureshi MH, Harmsen AG, Garvy BA. IL-10 Modulates Host Responses and Lung Damage Induced by Pneumocystis carinii Infection. The Journal of Immunology. 2003;170(2):1002.

98. Roy MG, Livraghi-Butrico A, Fletcher AA, McElwee MM, Evans SE, Boerner RM, et al. Muc5b is required for airway defence. Nature. 2014;505(7483):412-6.

99. Rojas DA, Iturra PA, Méndez A, Ponce CA, Bustamante R, Gallo M, et al. Increase in secreted airway mucins and partial Muc5b STAT6/FoxA2 regulation during Pneumocystis primary infection. Scientific Reports. 2019;9(1):2078.

100. Hao Y, Kuang Z, Jing J, Miao J, Mei LY, Lee RJ, et al. Mycoplasma pneumoniae modulates STAT3-STAT6/EGFR-FOXA2 signaling to induce overexpression of airway mucins. Infection and immunity. 2014;82(12):5246-55.

101. Gauguet S, Ortona S, Ahnger-Pier K, Duan B, Surana NK, Lu R, et al. Intestinal Microbiota of Mice Influences Resistance to Staphylococcus aureus Pneumonia. Infection and Immunity. 2015;83(10):4003.